

2.2 CE-TOFMS analysis and data processing

CE-TOFMS analysis was performed by an Agilent CE system combined with a TOFMS (Agilent Technologies, Palo Alto, CA, USA) as described previously (Ohashi et al. 2008) with slight modifications. Cationic metabolites were separated through a fused silica capillary (50 μm internal diameter \times 80 cm total length) preconditioned with a commercial buffer (H3301-1001, Human Metabolome Technologies Inc. (HMT), Tsuruoka, Japan) and filled with 1 M formic acid as electrolyte, and a commercial sheath liquid (H3301-1020, HMT) was delivered at a rate of 10 $\mu\text{l}/\text{min}$. Sample solution was injected at a pressure of 50 mbar for 10 s. The applied voltage was set at 30 kV. Electrospray ionization-mass spectrometry (ESI-MS) was conducted in the positive-ion mode and the capillary and fragmentor voltages were set at 4,000 and 120 V, respectively. Nebulizer pressure was configured at 5 psig and N_2 was delivered as a drying gas at a rate of 7 l/min at 300 $^\circ\text{C}$. Exact mass data were acquired at the rate of 1.5 cycles/s over a 50–1,000 m/z range. Anionic metabolites were analyzed also through the fused silica capillary preconditioned with a commercial buffer (H3302-1022, HMT) and filled with 50 mM ammonium acetate solution (pH 8.5) as electrolyte, and the aforementioned sheath liquid was delivered at a rate of 10 $\mu\text{l}/\text{min}$. Sample solution was injected at a pressure of 50 mbar for 6 s. The nebulizer pressure, drying gas and its flow rate, applied voltage, and scanning condition of the spectrometer were configured in the same manner as the cationic metabolite analysis. ESI-MS was conducted in the negative mode, and the capillary and fragmentor voltages were set at 3,500 and 125 V, respectively. The data obtained by CE-TOFMS analysis were preprocessed using our proprietary automatic integration software, MasterHands. Each metabolite was identified and quantified based on the peak information including m/z , migration time, and peak area. The quantified data were then evaluated for statistical significance by Wilcoxon signed-rank test.

2.3 Enrichment of phosphopeptides

Sample tissues were disrupted by multi-beads shocker and suspended in 100 mM Tris-HCl (pH 9.0) containing 8 M urea, protein phosphatase inhibitors and protein phosphatase inhibitors cocktails (Sigma, St. Louis, MO, USA). After centrifugation at $1,500\times g$ for 10 min, the supernatant was reduced with 1 mM dithiothreitol, alkylated with 5 mM iodoacetamide, and then digested with Lys-C endopeptidase at 37 $^\circ\text{C}$ for 3 h, followed by 5-fold dilution with 50 mM ammonium bicarbonate and digestion with trypsin at 37 $^\circ\text{C}$ overnight. The digested samples were desalted using StageTips with SDB-XC Empore disk

membranes (3 M, St. Paul, MN, USA) (Rappsilber et al. 2003).

Phosphopeptides were enriched with hydroxy acid-modified metal oxide chromatography (HAMMOc) (Kyono et al. 2008; Sugiyama et al. 2007). Briefly, custom-made metal oxide chromatography tips were prepared using C8-StageTips and titania beads as described previously (Rappsilber et al. 2007). Prior to loading samples, the tips were equilibrated with 0.1 % trifluoroacetic acid (TFA), 80 % acetonitrile and 300 mg/ml lactic acid (solution A). The digested samples from normal or tumor tissues were diluted with 100 μl solution A and loaded into the HAMMOc tips. After successive washing with solution A and solution B (0.1 % TFA and 80 % acetonitrile), 0.5 % piperidine was used for elution. The eluted fraction was acidified with TFA, desalted using SDB-XC-Stage-Tips, and concentrated in a vacuum evaporator, followed by the addition of solution A for subsequent nanoLC-MS/MS analysis. The phosphopeptide enrichment and sample pretreatment was conducted in duplicate.

2.4 NanoLC-MS/MS analysis and database search

NanoLC-MS/MS analyses were conducted using LTQ-Orbitrap (Thermo Fisher Scientific, Rockwell, IL, USA), a Dionex Ultimate 3000 pump (Thermo Fisher Scientific) and an HTC-PAL autosampler (CTC Analytics, Zwingen, Switzerland). A self-pulled needle (150 mm length \times 100 μm internal diameter, 6- μm opening) packed with ReproSil C18 materials (3 μm , Dr. Maisch, Ammerbuch, Germany) was used as an analytical column with “stone-arch” frit (Ishihama et al. 2002). A polytetrafluoroethylene-coated column holder (Nikkoy Technos, Tokyo, Japan) was mounted on an x - y - z nanospray interface, and a tee connector with a magnet was used to hold the column needle and to set the appropriate spray position. The injection volume was 5 μl and the flow rate was 500 nl/min for the gradient separation of peptides (Ishihama 2005). The mobile phases consisted of (A) 0.5 % acetic acid and (B) 0.5 % acetic acid and 80 % acetonitrile. A three-step linear gradient of 5–10 % B in 5 min, 10–40 % B in 60 min, 40–100 % B in 5 min and 100 % B in 10 min was used. A spray voltage of 2,400 V was applied via the tee connector. The MS scan range was m/z 300–1,500 and the top ten precursor ions were selected for subsequent MS/MS scans. Resolution setting and its maximum injection time were configured at 60,000 and 500 ms, respectively. We also configured the normalized collision energy at 35.0, the isolation width at two, and the minimum signal at 500. Automatic gain controls were set at 500,000 in the MS analysis and at 10,000 in the MS/MS analysis. The capillary temperature was set at 200 $^\circ\text{C}$. A lock mass function was used with a peak derived from polydimethylsiloxane

as a lock mass for the LTQ-Orbitrap to obtain constant mass accuracy during gradient analysis (Olsen et al. 2005). Mass Navigator version 1.2 (Mitsui Knowledge Industry, Tokyo, Japan) was used to create peak lists on the basis of the recorded fragmentation spectra. Peptides and proteins were identified by means of automated database searching using Mascot (Matrix Science, London, UK) against UniProt/Swiss-Prot.

3 Results and discussion

3.1 Overall metabolomic profile and amino acids

We analyzed metabolomic profiles of normal and tumor tissues obtained from nine lung and seven prostate cancer patients by using CE-TOFMS. Based on their *m/z* values and migration times, 114 and 86 metabolites were measured in the lung and prostate tissues, respectively (Supplementary Table S1), and visualized on a metabolome-wide pathway map (Supplementary Fig. S1) using VANTED software (Junker et al. 2006). The metabolomic data were then normalized and hierarchically clustered on both the metabolite and sample axes for a heat map representation (Supplementary Fig. S2) and further analyzed by principal component analysis (PCA) using MeV software (Saeed et al. 2003). Thirty-nine metabolites including glycolytic and TCA cycle intermediates, amino acids, and purine nucleoside phosphates, were absolutely quantified (Supplementary Table S2). PCA indicated that tumor metabolomic profiles were much more heterogeneous than their normal counterparts and comprised multiple clusters (Fig. 1a). With reference to the patient information (Table 1) and the hierarchically-clustered samples (Supplementary Fig. S2), tumor types appeared to play a greater part than tumor stage or differentiation status in altering the overall metabolomic profile in lung cancer, whereas differentiation status contributed more in prostate cancer. Indeed, the cluster of squamous cell carcinoma (SCC) patients (L1–3 and L7) was well-distinguished from that of adenocarcinoma (L4, L6 and L9) and pleomorphic carcinoma (L5). This may reflect the intrinsic pathological difference that adenocarcinoma cells but not squamous carcinoma cells retain their function of secreting mucus as glandular epithelial cells. In prostate samples, poorly differentiated prostate tumors (P2–4) were distant from the cluster of moderately differentiated (P1 and P5–7) tumors, which overlapped with that of normal samples. This may be due to higher duct-forming capacity and hormone response of well-differentiated prostate tumors, as well as normal prostate cells, than that of poorly differentiated tumors.

Both lung and prostate tumor samples were well-separated primarily along the PC1 axis; thus, factor loadings for the PC1 axis were evaluated. Correlations with the PC1 were particularly high in branched-chain amino acids (BCAAs) such as Val ($R = -0.97$), Ile (-0.97), and Leu (-0.89) in lung, and Leu (-0.87) in prostate samples (Supplementary Fig. S3). BCAAs are known to be avidly taken up by tumors and highly oxidized in cancer patients (Baracos and Mackenzie 2006), and thus may serve as effective indicators for diagnosing lung tumors. In fact, average lung tumor concentrations of all the 19 amino acids measured were higher than their respective normal levels, as were average prostate tumor levels of all the amino acids except Asp, Ile and Met (Fig. 1b). This is possibly due to hyperactivity of protein degradation and amino acid transporters in tumor cells (Fuchs and Bode 2005; Vander Heiden et al. 2009). Although average tumor levels of most amino acids in lung samples were significantly higher than their respective normal levels, normal and tumor Asp levels were comparable. Asp may be actively consumed as a precursor for nucleic acids and these TCA cycle intermediates, because tumor concentrations of malate, fumarate and succinate were significantly higher than the normal levels. In prostate tissues, levels of some amino acids such as Asn, Lys, Phe, Ser and Tyr and total essential amino acids were particularly higher in poorly differentiated tumors (P2–4; black in Fig. 1b) than moderately differentiated tumors (P1 and P5–7; gray in Fig. 1b), of which levels were comparable to the corresponding normal levels (Fig. 1b), implying enhancement of acquiring the amino acids upon dedifferentiation of prostate cancer cells.

3.2 Energy charge and adenosine and guanosine phosphates

Adenylate and guanylate energy charges ($(([RTP] + 0.5 \times [RDP])/([RTP] + [RDP] + [RMP]))$, $R = A$ or G) were lower in lung tumor than normal tissues (Fig. 2a); however, tumor levels were significantly higher than normal levels for ATP (3.8-fold), GTP (4.2-fold), and the other adenosine and guanosine phosphates (1.9–7.9-fold), and hence total adenylates (4.5-fold) and guanylates (4.0-fold). Tumor concentrations of these metabolites were relatively higher in all the SCC samples (L1–3 and L7; black in Fig. 2a) than the others (gray in Fig. 2a) such as L5 and L6, whose overall tumor metabolomic profiles resembled their respective normal profiles (Fig. 1). Purine synthesis may thus be hyperactivated in lung tumors, especially SCC, probably with a high basal $ATP \leftrightarrow ADP$ turnover and purine salvage for maximizing their growth. Although prostate tissues showed much less normal-versus-tumor

differences, tumor ADP level was significantly lower than normal level (Fig. 2b). High absolute concentrations of ADP and GDP among other purine nucleoside phosphates are unique to prostate tissues, and ATP and AMP levels were relatively higher in poorly differentiated tumors (P2–4; black in Fig. 2b) than moderately differentiated tumors (P1 and P5–7; gray in Fig. 2b). This might be due to a differential expression of adenylate kinase catalyzing the reaction, $2\text{ADP} \leftrightarrow \text{ATP} + \text{AMP}$, which is undetectable in adult prostate but shows activity along with its malignant alteration (Hall et al. 1985).

3.3 Glycolytic and TCA cycle intermediates and phosphorylated enzymes

Most glycolytic and TCA cycle intermediates were absolutely quantified (Fig. 3a), and phosphorylation levels of associated enzymes were also examined (Fig. 3b). Tumor lactate levels were higher than normal levels in both lung and prostate tissues, indicating their enhanced glycolysis and lactate fermentation, which reaffirmed the Warburg effect in cancer. Lung tumor levels of fructose 6-phosphate and fructose 1,6-bisphosphate were significantly lower and higher, respectively, than their corresponding normal levels. This may be partly explained by significantly high tumor levels of S386 phosphorylation in phosphofructokinase, which enhances its activity (Brand and Soling 1975), and thus the overall glycolytic flux because it is a

bottleneck enzyme. Although tumor levels of S83 phosphorylation in glyceraldehyde 3-phosphate dehydrogenase and S203 in phosphoglycerate kinase-1 were significantly higher than their respective normal levels, their functional impacts are unknown. Tumor level of S37 phosphorylation of pyruvate kinase, which enhances its activity (Le Mellay et al. 2002), was significantly higher than the normal level. This may rationalize the trend that phosphoenolpyruvate and pyruvate were significantly lower and higher, respectively, in tumor than normal tissues. Tumor levels of S293 and S291 phosphorylation in pyruvate dehydrogenase, which inhibit its activity (Korotchkina and Patel 2001; Patel and Korotchkina 2001), were significantly higher than normal levels in all the lung cancer patients, except L6. This inhibition may contribute to the enhanced glycolysis and resulting lactate accumulation in lung tumors. In prostate tissues, however, most glycolytic intermediates were not detected, probably owing to inevitable over-dilution of the samples for reducing polyamine concentrations, which otherwise adversely interfere with CE-TOFMS analysis. Trivial differences were observed between normal and tumor prostate phosphorylation levels of most glycolytic enzymes except glucose 6-phosphate isomerase (G6PI); nevertheless, the impact of elevated phosphorylation on the activity of G6PI is uncertain. Although intriguing, there was no apparent correlation between significantly high tumor levels of S481 phosphorylation in ATP citrate lyase in SCC samples, L1, L3

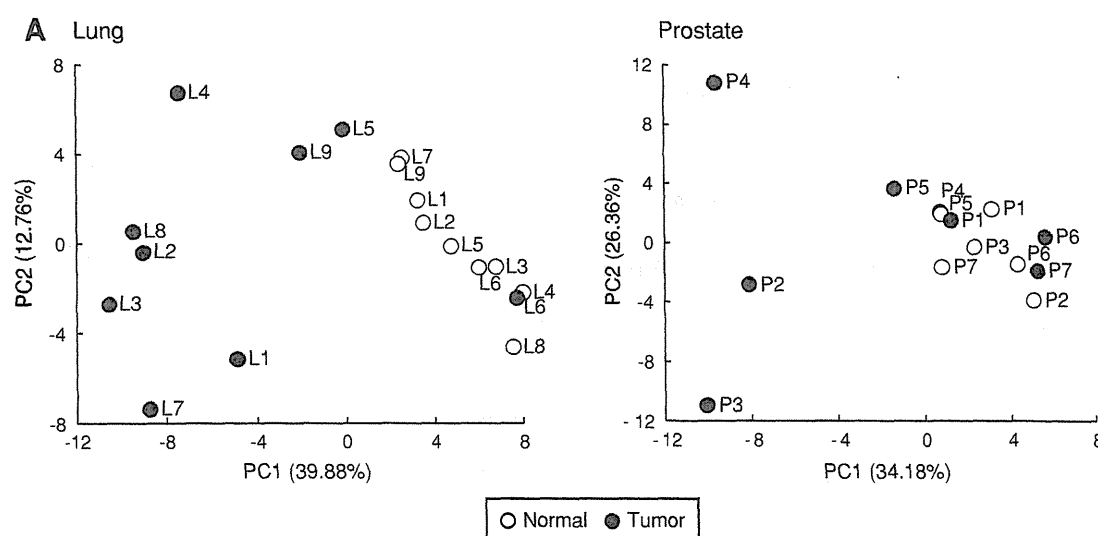


Fig. 1 **a** Score plots of PCA using the normalized metabolomic data of paired normal and tumor tissues obtained from lung (*left*) and prostate (*right*) cancer patients. The sample codes correspond to the patient IDs listed in Table 1. *Percentage values* indicated on the axes represent the contribution rate of the first (PC1) and the second (PC2) principal components. **b** Quantified levels of amino acids in normal (*left, open dots*) and tumor (*right, filled dots*) tissues obtained from lung and prostate cancer patients. *Horizontal bars* represent mean \pm SD of

normal (*left*) and tumor (*right*) samples and each connected pair represents the values for the same patient. *Gray dots* represent the values for patients with non-SCC lung cancer (L4–L6, L8 and L9) and patients with moderately differentiated prostate cancer (P1 and P5–7). *N.D.* indicates that the metabolite level was below the detection limit of the analysis. *Asterisks* indicate the significant differences between normal and tumor tissue levels based on the Wilcoxon signed-rank test (* $p < 0.05$; ** $p < 0.01$; and *** $p < 0.001$)

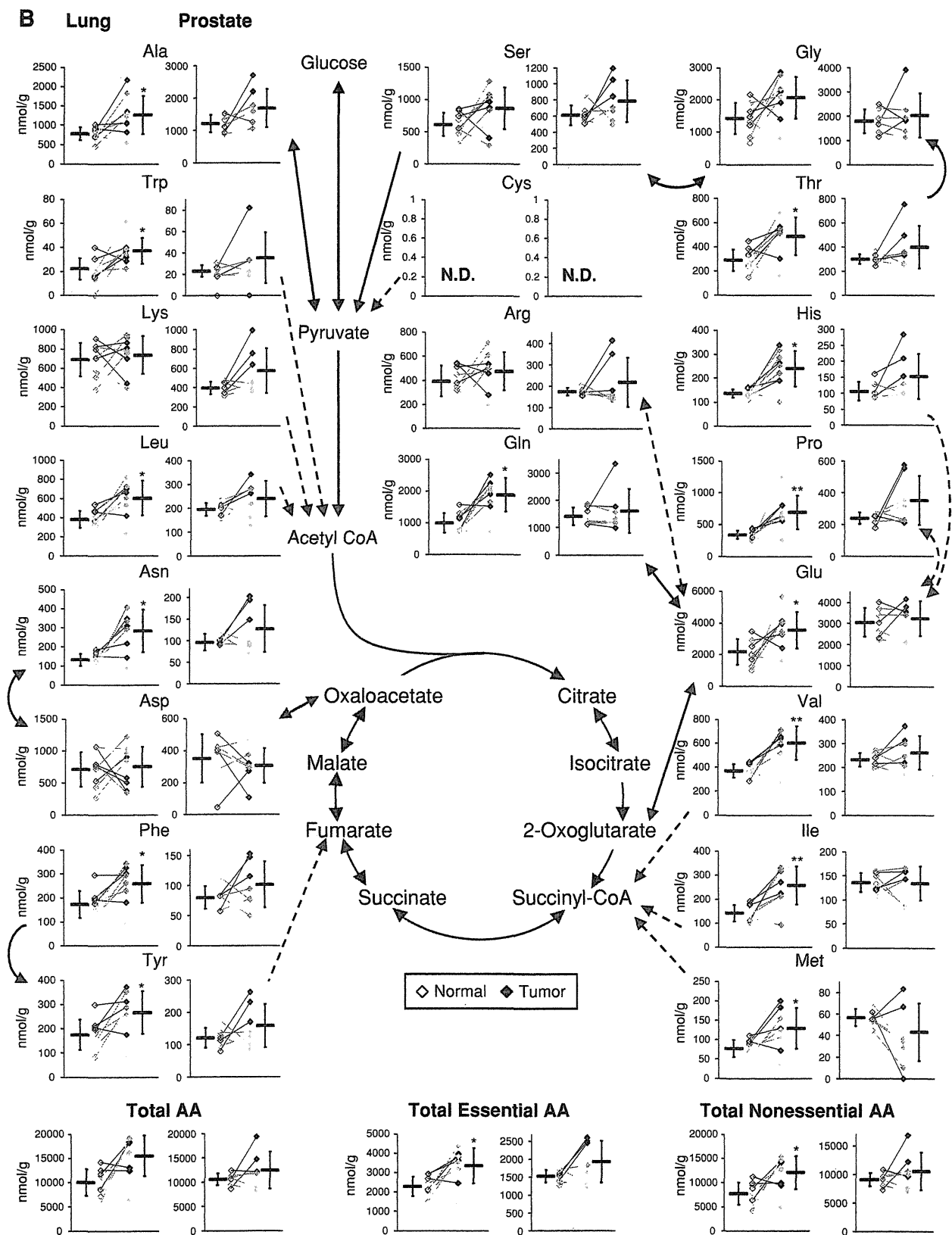


Fig. 1 continued

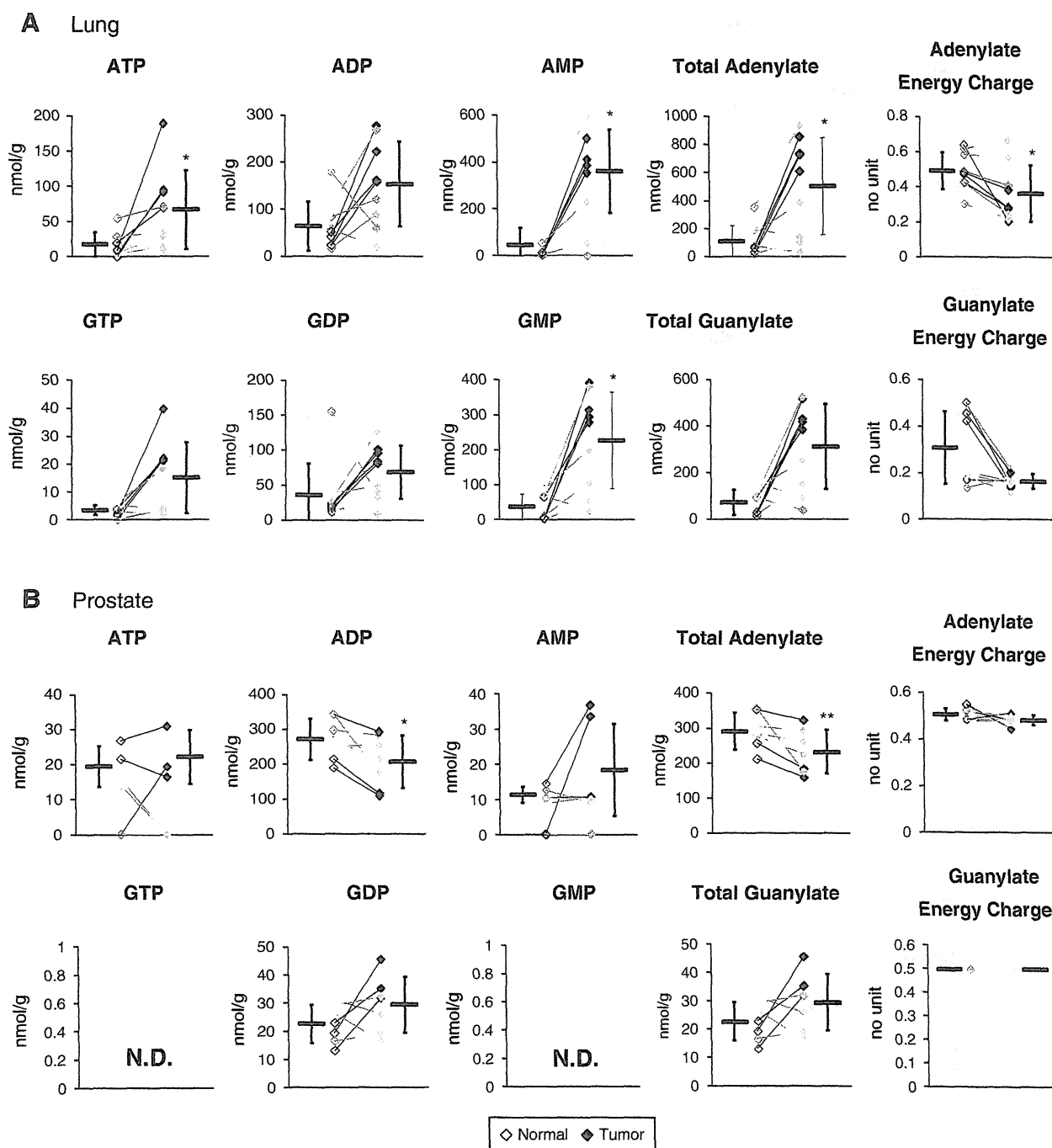
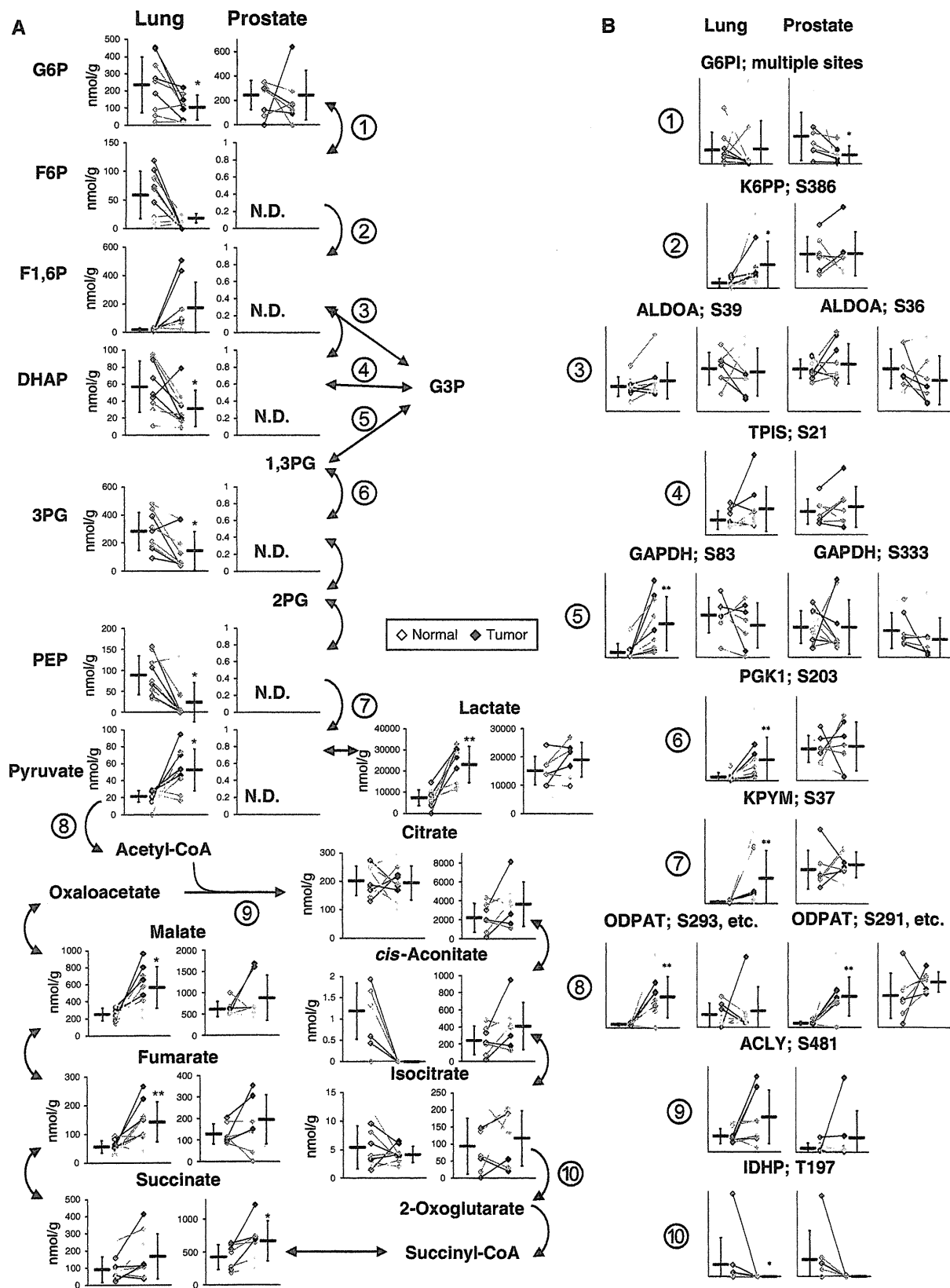


Fig. 2 Adenosine and guanosine phosphates, total adenylates and guanylates, and adenylate and guanylate energy charges of normal (left, open dots) and tumor (right, filled dots) tissues obtained from lung (a) and prostate (b) cancer patients. Horizontal bars represent mean \pm SD of normal (left) and tumor (right) samples and each connected pair represents the values for the same patient. Gray dots represent the values for patients with non-SCC lung cancer (L4–L6,

L8 and L9) and patients with moderately differentiated prostate cancer (P1 and P5–7). *N.D.* indicates that the metabolite level was below the detection limit of the analysis. Asterisks indicate the significant differences between normal and tumor tissue levels based on the Wilcoxon signed-rank test (* $p < 0.05$; ** $p < 0.01$; and *** $p < 0.001$)



◀ **Fig. 3** Quantified levels of glycolytic and TCA cycle intermediates (a) and phosphorylation levels of each phosphorylation site in associated enzymes (b) in normal (left, open dots) and tumor (right, filled dots) tissues obtained from lung and prostate cancer patients. Encircled numbers in (a) indicated next to the metabolic reactions involved in glycolysis and the TCA cycle correspond to the associated enzymes in (b). Horizontal bars represent mean \pm SD of normal (left) and tumor (right) samples and each connected pair represents the values for the same patient. Gray dots represent the values for patients with non-SCC lung cancer (L4–L6, L8 and L9) and patients with moderately differentiated prostate cancer (P1 and P5–7). N.D. indicates that the metabolite level was below the detection limit of the analysis. Asterisks indicate the significant differences between normal and tumor tissue levels based on the Wilcoxon signed-rank test (* $p < 0.05$; ** $p < 0.01$; and *** $p < 0.001$). *G6PI* glucose 6-phosphate isomerase; *K6PP* 6-phosphofructokinase; *ALDOA* aldolase A; *TPIS* triosephosphate isomerase; *GAPDH* glyceraldehydes 3-phosphate dehydrogenase; *PGKI* phosphoglycerate kinase 1; *KPYM* pyruvate kinase isozymes M1/M2; *ODPAT* pyruvate dehydrogenase E1 component subunit alpha; *ACLY* ATP-citrate synthase; and *IDHP* isocitrate dehydrogenase

and L7, and their citrate concentrations. The impact of elevated phosphorylation levels of T197 in isocitrate dehydrogenase in normal L2 and P2 samples was also unclear. We need a larger number of sample sets in order to validate these results and provide further insight into possible correlations between phosphorylated states of the enzymes and metabolomic profiles.

Levels of all the quantified TCA cycle intermediates were higher in tumor than normal prostate tissues (Fig. 3a), which may be related to the typically hypoxic microenvironment of prostate tissues, because most TCA cycle intermediates are known to increase under hypoxia, while their flux through the pathway remains low (Wiebe et al. 2008). Average prostate citrate concentrations were >11-fold higher than in lung. This was partly due to a high concentration of zinc in the prostate, which inhibits m-aconitase and results in citrate accumulation (Mycielska et al. 2009). Prostate tumor exhibits low zinc levels and elevated fatty acid synthesis consuming citrate, and thus its citrate level is typically lower than in normal tissues (Mycielska et al. 2009), which is, however, inconsistent with our results. Tumor citrate, *cis*-aconitate, and isocitrate levels in P1, P3 and P7 were consistently lower than their respective normal levels, leaving the possibility that zinc and m-aconitase activity levels may vary depending on a factor other than differentiation status.

Succinate, fumarate, and malate levels were markedly higher in both prostate and lung tumor tissues than their corresponding normal tissues (Fig. 3a), which was consistent with our previous results for colon and stomach tumor metabolomics (Hirayama et al. 2009). We recently obtained strong evidence that, especially under hypoxic and nutrient-deprived conditions, energy generation of cancer relies on fumarate respiration (Sakai et al. 2012;

Tomitsuka et al. 2010). This confers upon cells the ability to produce ATP by harnessing fumarate to succinate conversion, rather than oxygen to water, as the final electron transport step via the reverse reaction of succinate dehydrogenase (Kita and Takamiya 2002). Accumulation of these metabolites in tumors may therefore be attributed to hyperactivity of fumarate respiration.

3.4 Tumor-specificity and organ-dependency in metabolite profiles

The metabolome data obtained from both lung and prostate tissues were collectively normalized and hierarchically clustered (Supplementary Fig. S4A). As a result, lung-versus-prostate differences in terms of the overall metabolomic profiles appeared to be more significant than normal-versus-tumor differences within the same organ, as observed in our previous comparative metabolome analyses in colon and stomach tissues (Hirayama et al. 2009). As expected, PCA with the collectively normalized data showed clear inter-organ differences along with the PC2 axis; however, the normal-versus-tumor distinctions were also observed along with the PC1 axis (Supplementary Fig. S4B). This suggests that, in the carcinogenic process, cells alter their metabolism with a certain ‘metabolic directionality’ that is independent of organ types while retaining much of the metabolism that is unique to their organs of origin. Metabolites that showed high correlations with the PC2 included several nucleosides, TCA cycle intermediates, and polyamines, which characterize the inter-organ metabolic differences (Supplementary Table S3). In contrast, most glucogenic amino acids such as Thr, Ile, Asn, Pro, His, Gln, and Ser were closely associated with the PC1 (Supplementary Table S3), suggesting that a hyper-production and/or -acquisition of a certain set of amino acids likely occurs in the course of tumorigenesis.

4 Conclusion

Overall tumor metabolomic profiles were found to be significantly different depending on tumor type in lung cancer and differentiation status in prostate cancer. Elevated tumor concentrations of almost all the amino acids, especially BCAAs, were identified in an organ-independent manner, and this trend was more prominent in SCC than the other tumor types in lung cancer and in poorly rather than moderately differentiated prostate cancer. Analyses with much more samples, however, are necessary in order to statistically confirm these unique subtype-specific metabolic fingerprint of cancer. In contrast, through our combined metabolomic and phosphorylated enzyme analyses, we found that glycolytic and TCA cycle intermediates,

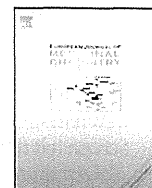
levels of which are probably associated with enzyme phosphorylation levels, exhibited significant organ dependency, reaffirming that inter-organ metabolomic differences are generally more significant than normal-versus-tumor differences within the same organ. Nonetheless, metabolomic profiles of both lung and prostate tumors appear to have a common 'directionality' along with their increasing malignancy represented by high concentrations of a certain set of glucogenic amino acids. Taken together, we identified organ-dependent, tumor-specific, and tumor-pathology-dependent metabolic features, which highlights the need for a combined metabolomics and phosphoproteomics analysis on a broader scale with a larger number of sample sets for improving specificity and effectiveness of personalized anticancer therapeutics.

Acknowledgments The authors thank Dr. Masahiro Sugimoto for developing MasterHands software. This work was supported in part by a grant for the Third Term Comprehensive 10-year Strategy for Cancer Control from the Ministry of Health, Labour and Welfare (H.E.) and a grant from the Global COE Program entitled, "Human Metabolomic Systems Biology" (K.K.). This work was also supported by KAKENHI (Grant-in-Aid for Scientific Research) on Priority Areas "Systems Genomes" and on "Lifesurveyor" from the Ministry of Education, Culture, Sports, Science and Technology (MEXT) of Japan as well as research funds from the Yamagata prefectural government and the City of Tsuruoka (Y.O., M.T., and T.S.).

Open Access This article is distributed under the terms of the Creative Commons Attribution License which permits any use, distribution, and reproduction in any medium, provided the original author(s) and the source are credited.

References

- Baracos, V. E., & Mackenzie, M. L. (2006). Investigations of branched-chain amino acids and their metabolites in animal models of cancer. *Journal of Nutrition*, 136, 237S–242S.
- Brand, I. A., & Soling, H. D. (1975). Activation and inactivation of rat liver phosphofructokinase by phosphorylation–dephosphorylation. *FEBS Letters*, 57, 163–168.
- Fuchs, B. C., & Bode, B. P. (2005). Amino acid transporters ASCT2 and LAT1 in cancer: Partners in crime? *Seminars in Cancer Biology*, 15, 254–266.
- Hall, M., Mickey, D. D., Wenger, A. S., & Silverman, L. M. (1985). Adenylate kinase: An oncogene marker in an animal model for human prostatic cancer. *Clinical Chemistry*, 31, 1689–1691.
- Heiden, M. G. V., Cantley, L. C., & Thompson, C. B. (2009). Understanding the Warburg effect: The metabolic requirements of cell proliferation. *Science*, 324, 1029–1033.
- Hirayama, A., Kami, K., Sugimoto, M., Sugawara, M., Toki, N., Onozuka, H., et al. (2009). Quantitative metabolome profiling of colon and stomach cancer microenvironment by capillary electrophoresis time-of-flight mass spectrometry. *Cancer Research*, 69, 4918–4925.
- Ishihama, Y. (2005). Proteomic LC-MS systems using nanoscale liquid chromatography with tandem mass spectrometry. *Journal of Chromatography A*, 1067, 73–83.
- Ishihama, Y., Rappsilber, J., Andersen, J. S., & Mann, M. (2002). Microcolumns with self-assembled particle frits for proteomics. *Journal of Chromatography A*, 979, 233–239.
- Junker, B. H., Klukas, C., & Schreiber, F. (2006). VANTED: A system for advanced data analysis and visualization in the context of biological networks. *BMC Bioinformatics*, 7, 109.
- Kita, K., & Takamiya, S. (2002). Electron-transfer complexes in *Ascaris* mitochondria. *Advances in Parasitology*, 51, 95–131.
- Korotchkina, L. G., & Patel, M. S. (2001). Site specificity of four pyruvate dehydrogenase kinase isoenzymes toward the three phosphorylation sites of human pyruvate dehydrogenase. *Journal of Biological Chemistry*, 276, 37223–37229.
- Kyono, Y., Sugiyama, N., Imami, K., Tomita, M., & Ishihama, Y. (2008). Successive and selective release of phosphorylated peptides captured by hydroxy acid-modified metal oxide chromatography. *Journal of Proteome Research*, 7, 4585–4593.
- Le Mellay, V., Houben, R., Troppmair, J., Hagemann, C., Mazurek, S., Frey, U., et al. (2002). Regulation of glycolysis by Raf protein serine/threonine kinases. *Advances in Enzyme Regulation*, 42, 317–332.
- Mycielska, M. E., Patel, A., Rizaner, N., Mazurek, M. P., Keun, H., Ganapathy, V., et al. (2009). Citrate transport and metabolism in mammalian cells: Prostate epithelial cells and prostate cancer. *BioEssays*, 31, 10–20.
- Ohashi, Y., Hirayama, A., Ishikawa, T., Nakamura, S., Shimizu, K., Ueno, Y., et al. (2008). Depiction of metabolome changes in histidine-starved *Escherichia coli* by CE-TOFMS. *Molecular BioSystems*, 4, 135–147.
- Olsen, J. V., de Godoy, L. M., Li, G., Macek, B., Mortensen, P., Pesch, R., et al. (2005). Parts per million mass accuracy on an Orbitrap mass spectrometer via lock mass injection into a C-trap. *Molecular and Cellular Proteomics*, 4, 2010–2021.
- Patel, M. S., & Korotchkina, L. G. (2001). Regulation of mammalian pyruvate dehydrogenase complex by phosphorylation: Complexity of multiple phosphorylation sites and kinases. *Experimental & Molecular Medicine*, 33, 191–197.
- Rappsilber, J., Ishihama, Y., & Mann, M. (2003). Stop and go extraction tips for matrix-assisted laser desorption/ionization, nanoelectrospray, and LC/MS sample pretreatment in proteomics. *Analytical Chemistry*, 75, 663–670.
- Rappsilber, J., Mann, M., & Ishihama, Y. (2007). Protocol for micro-purification, enrichment, pre-fractionation and storage of peptides for proteomics using StageTips. *Nature Protocols*, 2, 1896–1906.
- Saeed, A. I., Sharov, V., White, J., Li, J., Liang, W., Bhagabati, N., et al. (2003). TM4: A free, open-source system for microarray data management and analysis. *BioTechniques*, 34, 374–378.
- Sakai, C., Tomitsuka, E., Esumi, H., Harada, S., & Kita, K. (2012). Mitochondrial fumarate reductase as a target of chemotherapy: From parasites to cancer cells. *Biochimica et Biophysica Acta*, 1820, 643–651.
- Sugiyama, N., Masuda, T., Shinoda, K., Nakamura, A., Tomita, M., & Ishihama, Y. (2007). Phosphopeptide enrichment by aliphatic hydroxy acid-modified metal oxide chromatography for nano-LC-MS/MS in proteomics applications. *Molecular and Cellular Proteomics*, 6, 1103–1109.
- Tomitsuka, E., Kita, K., & Esumi, H. (2010). The NADH-fumarate reductase system, a novel mitochondrial energy metabolism, is a new target for anticancer therapy in tumor microenvironments. *Annals of the New York Academy of Sciences*, 1201, 44–49.
- Warburg, O. (1956). On the origin of cancer cells. *Science*, 123, 309–314.
- Wiebe, M. G., Rintala, E., Tamminen, A., Simolin, H., Salusjarvi, L., Toivari, M., et al. (2008). Central carbon metabolism of *Saccharomyces cerevisiae* in anaerobic, oxygen-limited and fully aerobic steady-state conditions and following a shift to anaerobic conditions. *FEMS Yeast Research*, 8, 140–154.



Original article

Synthesis and antitumor evaluation of arctigenin derivatives based on antiausterity strategy

Naoki Kudou^a, Akira Taniguchi^b, Kenji Sugimoto^a, Yuji Matsuya^a, Masashi Kawasaki^c, Naoki Toyooka^{b,d,*}, Chika Miyoshi^e, Suresh Awale^f, Dya Fita Dibwe^g, Hiroyasu Esumi^e, Shigetoshi Kadota^g, Yasuhiro Tezuka^{g,**}

^a Graduate School of Medicine and Pharmaceutical Sciences, University of Toyama, 2630 Sugitani, Toyama, 930-0194, Japan

^b Graduate School of Science and Technology for Research, University of Toyama, 3190 Gofuku, Toyama 930-8555, Japan

^c Department of Liberal Arts and Sciences, Faculty of Engineering, Toyama Prefectural University, 5180 Kurokawa, Kosugi-Machi, Toyama 939-0398, Japan

^d Graduate School of Innovative Life Science, University of Toyama, 3190 Gofuku, Toyama 930-8555, Japan

^e Cancer Physiology Project, Research Center for Innovative Oncology, National Cancer Center Hospital East, Chiba, Japan

^f Frontier Research Core for Life Sciences, University of Toyama, 2630 Sugitani, Toyama 930-0194, Japan

^g Institute of Natural Medicine, University of Toyama, 2630 Sugitani, Toyama 930-0194, Japan

ARTICLE INFO

Article history:

Received 24 July 2012

Received in revised form

14 September 2012

Accepted 21 November 2012

Available online 28 November 2012

Keywords:

(–)-Arctigenin derivatives

Antiausterity activity

Synthesis

Pancreatic cancer

ABSTRACT

A series of new (–)-arctigenin derivatives with variably modified O-alkyl groups were synthesized and their preferential cytotoxicity was evaluated against human pancreatic cancer cell line PANC-1 under nutrient-deprived conditions. The results showed that monoethoxy derivative **4i** (PC₅₀, 0.49 μM), diethoxy derivative **4h** (PC₅₀, 0.66 μM), and triethoxy derivative **4m** (PC₅₀, 0.78 μM) showed the preferential cytotoxicities under nutrient-deprived conditions, which were identical to or more potent than (–)-arctigenin (**1**) (PC₅₀, 0.80 μM). Among them, we selected the triethoxy derivative **4m** and examined its *in vivo* antitumor activity using a mouse xenograft model. Triethoxy derivative **4m** exhibited also *in vivo* antitumor activity with the potency identical to or slightly more than (–)-arctigenin (**1**). These results would suggest that a modification of (–)-arctigenin structure could lead to a new drug based on the antiausterity strategy.

© 2012 Elsevier Masson SAS. All rights reserved.

1. Introduction

Pancreatic cancer is the most aggressive cancer of all and has an exceptionally high global mortality rate, with an estimated 267,000 deaths worldwide in 2008. It ranks 8th or 9th as the most frequent cause of cancer death worldwide and is the 4th or 5th most frequent cause of cancer death in most developed countries, including the United States, Europe, and Japan [1]. Moreover, it has been estimated that the number of deaths from pancreatic cancer will reach 484,000 by 2030 [1]. Pancreatic cancer rapidly metastasizes and lead the patients to die in a short period of the diagnosis. Thus, the 5-year survival rate of the patients with the pancreatic cancer is the lowest among several cancers [2,3]. Though surgery is the only treatment method that offers any prospect of potential cure, chemotherapy

with 5-fluorouracil and gemcitabine is also used for palliative therapy of advanced pancreatic cancer. However pancreatic cancer is largely resistant to most known chemotherapeutic agents including 5-fluorouracil and gemcitabine [4]. Therefore effective chemotherapeutic agents that target pancreatic cancer are urgently needed.

Tumor cells, in general, proliferate very fast, and the demand for essential nutrients, oxygen, etc. is always high. The immediate environment of cancers increasing in size, however, often becomes heterogeneous and some regions of large cancers often possess microenvironmental niches, which exhibit a significant gradient of critical metabolites including oxygen, glucose, other nutrients, and growth factors [5]. Thus, many cancer cells get the critical metabolites by randomly recruiting new blood vessels, a phenomenon commonly known as angiogenesis, to survive under such severe conditions. However, human pancreatic cancer survives with an extremely poor blood supply and becomes more malignant [6]. The method by which pancreatic cancer survives is by getting a remarkable tolerance to extreme nutrient starvation [7]. Therefore, it has been hypothesized that eliminating the tolerance of cancer cells to nutrition starvation

* Corresponding author. Graduate School of Science and Technology for Research, University of Toyama, 3190 Gofuku, Toyama 930-8555, Japan. Tel.: +81 76 445 6859.

** Corresponding author. Tel.: +81 76 434 7627; fax: +81 76 434 5059.

E-mail addresses: toyooka@eng.u-toyama.ac.jp (N. Toyooka), tezuka@inm.u-toyama.ac.jp (Y. Tezuka).

may allow a novel biochemical approach known as “anti-austerity” for cancer therapy [8].

In this regard, we screened 500 medicinal plants used in Kampo medicine to identify agents that preferentially reduce the survival of nutrient-deprived human pancreatic cancer PANC-1 cells. The screen led to the isolation of (–)-arctigenin (**1**) as the active principle of *Arctium lappa* [9]. In addition to pancreatic cancer, arctigenin has been reported to inhibit lung, skin, and stomach cancers [10]. Thus, we started the synthetic work of arctigenin derivatives to obtain more effective drugs against pancreatic cancer. In *A. lappa*, (–)-arctigenin is mainly contained as its glucoside, arctiin, and after consumption arctiin was reported to be deglucosidated to (–)-arctigenin (**1**), followed by demethylation and dehydroxylation by intestinal bacteria to metabolites I–V [11]. As reported previously, (–)-arctigenin showed potent preferential cytotoxicity, whereas its glucoside, arctiin, showed no cytotoxicity [9]. In our preliminary examination, moreover, metabolites I and V (Fig. 1) showed weaker activity. These facts should suggest that the 4'-hydroxyl group should be important for the preferential cytotoxicity and that (–)-arctigenin is deactivated through the demethylation/demethoxylation. In addition, the enantiomer of (–)-arctigenin (**1**), (+)-arctigenin (Fig. 1), showed very weak preferential cytotoxicity, indicating the importance of the 2*R*,3*R* absolute stereochemistry of (–)-form. Thus, with an intention to improve the metabolism stability, we have synthesized 15 arctigenin derivatives **4a–o** with different alkoxy substituent and the 2*R*,3*R*-configuration, and the *in vitro* preferential cytotoxicity of them was characterized under nutrient-deprived conditions. Then, the triethoxy derivative **4m**, exhibiting the *in vitro* activity identical to **1** and having no methoxy group which may be metabolized, was selected and further evaluated the effect against tumor cell growth *in vivo* in a cancer xenograft mouse model.

2. Results and discussion

2.1. Chemistry

First we planned the synthesis of derivatives on the 3' position of (–)-arctigenin. For this purpose, (–)-arctigenin (**1**) was converted to the diol **2** [12], which was transformed into 6 derivatives **4a–f** via selective protection of **2**, alkylation of **3**, followed by deprotection of the benzyl group (Scheme 1).

Next we planned the efficient and flexible synthesis of a variety of derivatives on the 3', 3'', and 4'' positions of (–)-arctigenin.

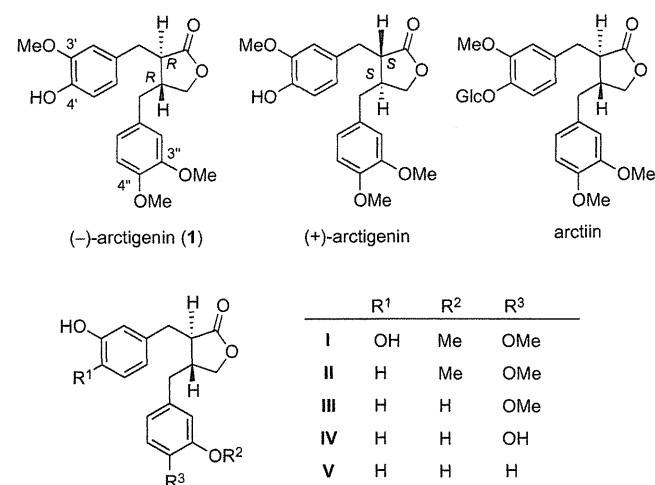


Fig. 1. Structures of (–)-arctigenin (**1**) and its analogs.

3,4-Dihydroxybenzaldehyde was converted to the alcohol **7** via known benzyl ether **5** [13] and aldehyde **6** [14]. Mono-alkylation of diethyl malonate with the mesylate of **7** afforded the ester **8**. Reduction of **8** and lipase-mediated transesterification of the resulting diol provided the mono-acetate (+)-**9**. The enantiomeric excess of (+)-**9** was determined to be 98% ee by the HPLC analysis using the chiral column (Chiralcel OJ). The absolute stereochemistry of (+)-**9** was determined by the comparison of the optical rotation with known lactone **13a**, prepared from (+)-**9** via mesylate **10**, benzyl ether **11**, and lactone **12a** as shown in Scheme 2. Other lactones **13b–f** were also prepared from (+)-**9**, and these lactones **13b–f** were alkylated on the α -position with several alkyl halides to afford the di-substituted lactones **14a–i**. Finally deprotection of the benzyl group furnished the desired derivatives **4g–o**.

From the comparison of the *in vitro* activity of the synthesized derivatives **4a–o** against the human pancreatic cancer cell line PANC-1, the triethoxy derivative **4m** was chosen as the potent candidate for the *in vivo* experiment. As the more effective synthesis of **4m**, we investigated the modified synthesis of the lactone **13d**. 3,4-Dihydroxybenzaldehyde was converted to the ester **17** via known aldehyde **15** [15] and alcohol **16** [16] as the same procedure for the synthesis of **8**. After reduction of **17**, lipase-mediated transesterification of the resulting diol afforded the mono-acetate **18**, whose enantiomeric excess was determined to be 98% ee again by the Mosher method. The mono-acetate **18** was then transformed into the lactone **13d** via mesylate **19** (Scheme 3).

2.2. *In vitro* preferential cytotoxicity of arctigenin derivatives

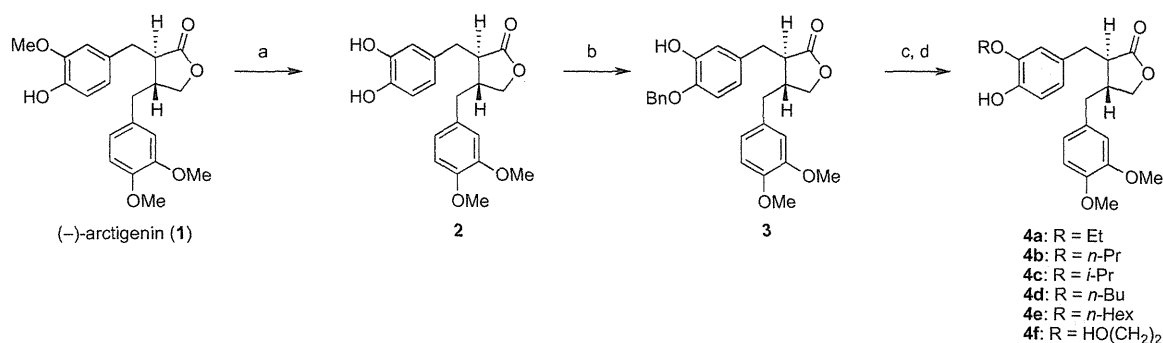
All of the (–)-arctigenin derivatives **4a–o** were evaluated for their *in vitro* preferential cytotoxic activity against human pancreatic cancer PANC-1 cells in nutrient-deprived medium (NDM). The PANC-1 cell line is highly resistant to nutrient starvation, and can survive in NDM even after 48 h of starvation [6,7,8]. However, this tolerance to nutrient starvation was remarkably eliminated by the tested compounds in a concentration-dependent manner. The tested compounds exhibited different potency of toxicity (Fig. 2) and their preferential cytotoxicities are obtained as the 50% cytotoxic concentration in NDM (PC₅₀ value) (Table 1). Among the (–)-arctigenin derivatives **4a–o**, monoethoxy derivative **4i** showed the most potent preferential cytotoxicity (PC₅₀, 0.49 μ M), followed by diethoxy derivative **4h** (PC₅₀, 0.66 μ M) and triethoxy derivative **4m** (PC₅₀, 0.78 μ M), which were identical to or more potent than (–)-arctigenin (**1**) (PC₅₀, 0.80 μ M).

On the relationship between the substituents and the preferential activity, the 3' position seems to favor smaller substituent since the PC₅₀ values of **1** and **4a–d** increase in the order: **1** (MeO) < **4a** (EtO) = **4b** (*n*-PrO) < **4c** (*i*-PrO) < **4d** (*n*-BuO). This would suggest the importance of the 4'-hydroxy group for the preferential activity. On the other hand, there is not clear relationship on the substituents at the 3'' and 4'' positions, although smaller substituents seems to be favor.

The order of *in vitro* preferential cytotoxicity (PC₅₀) was **4i** > **4h** > **4m**. Whereas **4h** and **4i** have the methoxy groups which was reported to be demethylated and then deoxygenated by intestinal bacteria and/or hepatic enzyme [11]. Thus, we selected the triethoxy derivative **4m** to pursue a further examination, from a viewpoint of metabolism stability.

2.3. *In vivo* antitumor activity of triethoxy derivative **4m**

The triethoxy derivative **4m** showed the *in vitro* preferential cytotoxicity also against human pancreatic cancer cell line CAPAN-1 under glucose deficient conditions with a intensity similar to (–)-arctigenin (**1**) (Fig. 3). We used PANC-1 cell line for *in vitro*

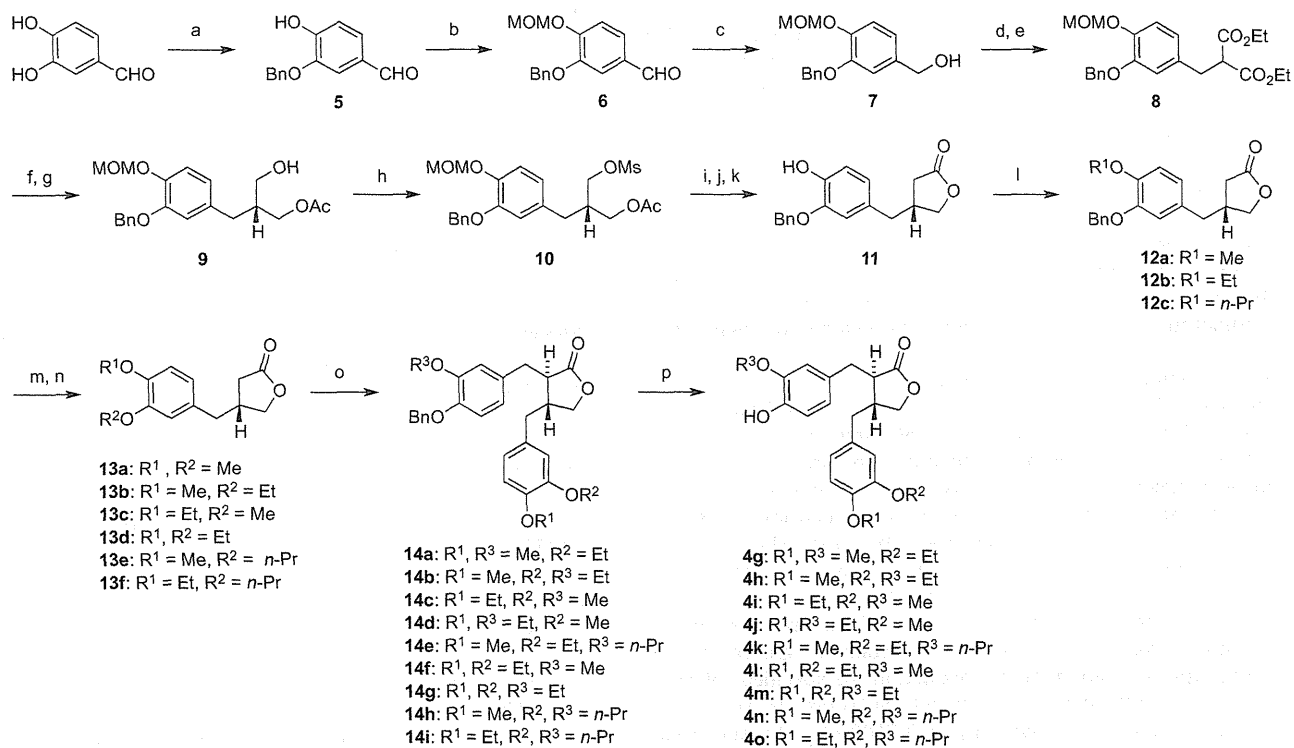


Scheme 1. Reagents and conditions: a: AlCl₃, pyridine, CH₂Cl₂, reflux (quant.); b: BnBr, K₂CO₃, KI, acetone, reflux (63%); c: RI or RBr, K₂CO₃, acetone, reflux for **4a–e** or 2-benzyloxyethanol, Ph₃P, DEAD, CH₂Cl₂, rt for **4f**; d: H₂, Pd(OH)₂, MeOH, rt.

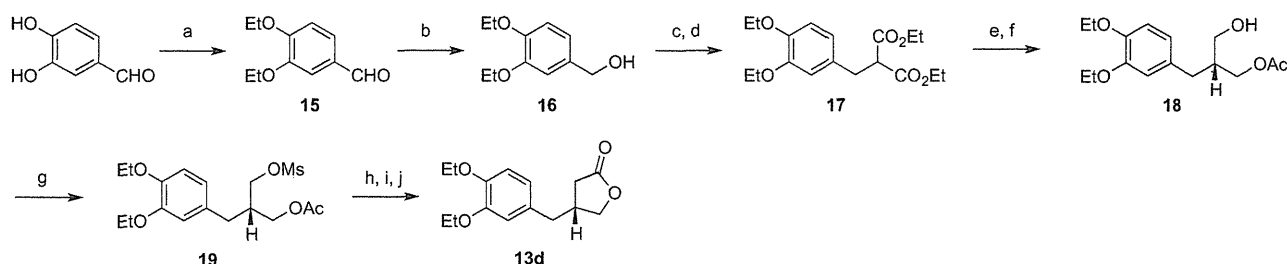
study because of its ready growth [17], while mouse xenograft model can be prepared with CAPAN-1 cell line more easily than with PANC-1 cell line [18]. Thus, we used mouse xenograft model with CAPAN-1 cell line for comparing the *in vivo* effect of triethoxy derivative **4m** with (–)-arctigenin (**1**).

Mice were inoculated with 5×10^6 CAPAN-1 cells s.c. on the back and then administered triethoxy derivative **4m**, (–)-arctigenin (**1**), or vehicle, as described in Experimental. The body weight of the animals was monitored weekly (Fig. 4A) and no significant body weight loss was recognized in the treated group versus the vehicle control group at any time during the experimental period. This fact, together with the behavior of the treated animals, indicated that

the tested compounds might have no toxicity at the dose used. The treatment was initiated from the 15th day by i.p. injection of the drug at the dose of 50 µg/mouse/d on 6 days of the week (or vehicle in the control group) until the 28th day. The tumor size was measured weekly. As is evident from the tumor growth curve shown in Fig. 4B, the tumor volume increased steadily in the control group, whereas the increase was significantly less prominent in the groups treated by triethoxy derivative **4m** or (–)-arctigenin (**1**). There was a significant difference in the tumor size at the day 21 between the groups treated by triethoxy derivative **4m** or (–)-arctigenin (**1**) and the control group ($P < 0.05$). Similarly, the mean wet weight and the size of the tumor were higher in the



Scheme 2. Reagents and conditions: a: BnBr, K₂CO₃, KI, acetone, reflux (64%); b: MOMCl, DIPEA, CH₂Cl₂, rt (quant.); c: NaBH₄, MeOH, rt (95%); d: MsCl, Et₃N, CH₂Cl₂, rt; e: diethyl malonate NaH, DMF, rt (72% in 2 steps); f: LiAlH₄, THF, reflux; g: lipase-PS (Amano), vinyl acetate, *i*-Pr₂O–THF rt (80% in 2 steps, 98% ee); h: MsCl, Et₃N, CH₂Cl₂, rt; i: KCN, DMSO, 90 °C; j: LiOH, THF–H₂O, rt; k: 10% NaOH (aq), reflux, then 10% HCl (aq)–THF, rt (73% in 4 steps); l: MeI or EtI or *n*-PrBr, K₂CO₃, acetone, reflux (88% for **12a**, 86% for **12b**, 87% for **12c**); m: H₂, Pd(OH)₂, MeOH; n: MeI or EtI, K₂CO₃, acetone, reflux (55% in 2 steps for **13a**, 55% in 2 steps for **13b**, 55% in 2 steps for **13c**, 47% in 2 steps for **13d**, 80% in 2 steps for **13e**, 77% in 2 steps for **13f**); o: LiHMDS, substituted BnBr, HMPA, THF, –78 °C to rt (44% for **14a**, 59% for **14b**, 43% for **14c**, 53% for **14d**, 40% for **14e**; 48% for **14f**; 56% for **14g**, 49% for **14h**; 33% for **14i**); p: H₂, Pd(OH)₂, MeOH (89% for **4g**, 63% for **4h**, 57% for **4i**, 63% for **4j**, 56% for **4k**, 81% for **4l**, 66% for **4m**, 46% for **4n**, 63% for **4o**).



Scheme 3. Reagents and conditions: a: EtI, K_2CO_3 , acetone, reflux (92%); b: $NaBH_4$, MeOH, rt (74%); c: MsCl, Et_3N , CH_2Cl_2 , rt; d: diethyl malonate NaH, DMF, rt (87% in 2 steps); e: $LiAlH_4$, THF, reflux; f: lipase-PS (Amano), vinyl acetate, i -Pr₂O–THF rt (53% in 2 steps, 98% ee); g: MsCl, Et_3N , CH_2Cl_2 , rt (79%); h: KCN, DMSO, 90 °C; i: LiOH, THF–H₂O, rt; j: 10% NaOH (aq), reflux, then 10% HCl (aq)–THF, rt (60% in 3 steps).

control group than the groups treated by triethoxy derivative **4m** or (–)-arctigenin (**1**) (Fig. 4C–F). These data indicate that triethoxy derivative **4m** also exerted antitumor activity *in vivo* with the potency identical to or slightly more than (–)-arctigenin (**1**).

3. Conclusion

In summary, a series of new (–)-arctigenin derivatives modified on *O*-alkyl groups were synthesized and their preferential cytotoxicity was evaluated against human pancreatic cancer cell line PANC-1 under nutrient-deprived conditions. The results showed that monoethoxy derivative **4i** (PC_{50} , 0.49 μ M), diethoxy derivative **4h** (PC_{50} , 0.66 μ M), and triethoxy derivative **4m** (PC_{50} , 0.78 μ M) showed the preferential cytotoxicities under nutrient-deprived conditions, which were identical to or more potent than (–)-arctigenin (**1**) (PC_{50} , 0.80 μ M). Among them, we selected the triethoxy derivative **4m** and examined *in vivo* antitumor activity with mouse xenograft model. Triethoxy derivative **4m** exhibited also *in vivo* antitumor activity with the potency identical to (–)-arctigenin (**1**). These results would suggest that a modification of (–)-arctigenin structure could lead to a new drug based on the antiausterity strategy.

4. Experimental

4.1. Chemistry

4.1.1. General conditions

Chemicals were purchased from Sigma–Aldrich, Merck, Nakalai Tesque, Wako Pure Chemicals, and Kanto Chemicals, and used without further purification. Column chromatography was done on Cica silica gel 60N (spherical, neutral; particle size, 40–50 μ m, Kanto Chemical Co., Inc., Tokyo, Japan), while thin-layer chromatography (TLC) was performed on Merck silica gel 60F₂₅₄ plates (Merck KGaA, Darmstadt, Germany). Melting points were taken on a Yanaco micromelting point apparatus and are uncorrected. The nuclear magnetic resonance (NMR) spectra were acquired in the specified solvent, in a Varian Gemini 300 spectrometer (300 and 75 MHz for ¹H and ¹³C, respectively) or Varian UNITY plus 500 spectrometer (500 and 125 MHz for ¹H and ¹³C, respectively) (Varian Inc., Palo Alto, CA, USA), with tetramethylsilane (TMS) as internal standard. The chemical shifts (δ) are reported in ppm downfield from TMS and coupling constants (*J*) are expressed in Hertz. Optical rotations were obtained in the specified solvent on a JASCO DIP-1000 digital polarimeter (JASCO Corp., Tokyo, Japan). IR spectra were measured with a JASCO FT/IR-460 Plus spectrophotometer (JASCO Corp.). The low-resolution mass spectra (MS) and high-resolution mass spectra (HRMS) were obtained with a Shimadzu GCMS-QP 500 mass spectrometer (Shimadzu Corp., Kyoto, Japan), JEOL D-200, or JEOL AX505 mass spectrometer (JEOL Ltd., Tokyo, Japan) in the electron impact mode at the ionization potential of 70 eV.

4.1.2. Synthesis of (–)-arctigenin derivatives **4a–4f**

4.1.2.1. (3*R*,4*R*)-3-(4-Benzyloxy-3-hydroxybenzyl)-4-(3,4-dimethoxybenzyl)dihydrofuran-2-one (3**).** To a stirred solution of (3*R*,4*R*)-3-(3,4-dihydroxybenzyl)-4-(3,4-dimethoxybenzyl)dihydrofuran-2-one (**2**) [12] (65.4 mg, 0.18 mmol) in acetone (2 mL) were added K_2CO_3 (37.3 mg, 0.27 mmol), KI (5.97 mg, 0.036 mmol), and BnBr (21.4 μ L, 0.18 mmol), and the resulting mixture was refluxed for 5 h. After cooling, the reaction mixture was filtered, and the filtrate was evaporated. The residue was chromatographed on silica gel (10 g, hexane:acetone = 4:1) to give **3** (51.2 mg, 63%) as a pale yellow oil: ¹H NMR (300 MHz, $CDCl_3$) δ : 1.60 (1H, br), 2.47–2.63 (4H, m), 2.86–2.98 (2H, m), 3.80 (3H, s), 3.85 (3H, s), 3.80–3.89 (1H, m), 4.09–4.14 (1H, m), 5.13 (2H, s), 6.47–6.80 (6H, m), 7.28–7.44 (5H, m); ¹³C NMR (75 MHz, $CDCl_3$) δ : 34.59, 38.19, 41.15, 46.53, 55.82, 55.98, 71.08, 71.21, 111.22, 111.72, 112.79, 113.95, 120.43, 121.20, 127.12, 127.69, 128.39, 130.30, 130.73, 136.98, 146.91, 147.67, 148.84, 149.63, 178.46; IR (neat): 1514 (C=C), 1769 (C=O) cm^{-1} ; MS (EI) *m/z* 449 (M^+); HRMS (EI): calcd for $C_{27}H_{28}O_6$: 448.1886 (M^+), found: 448.2743; $[\alpha]_D^{25}$ –20.7 (c 0.85, $CHCl_3$).

4.1.2.2. (3*R*,4*R*)-4-(3,4-Dimethoxybenzyl)-3-(3-ethoxy-4-hydroxybenzyl)dihydrofuran-2-one (4a**).** To a stirred solution of **3** (44.7 mg, 0.10 mmol) in acetone (5 mL) were added K_2CO_3 (82.6 mg, 0.60 mmol), EtI (26.5 μ L, 0.33 mmol), and the reaction mixture was refluxed for 48 h. After cooling, the reaction mixture was filtered, and the filtrate was evaporated. The residue was dissolved in MeOH (6 mL). To the solution was added 20% Pd(OH)₂ (10 mg), and the resulting suspension was stirred under a hydrogen atmosphere at 1 atm for 16 h. The catalyst was removed by filtration and the filtrate was evaporated. The residue was chromatographed on silica gel (7 g, hexane : acetone = 3:1) to give **4a** (13.4 mg, 35% in 2 steps) as a colorless oil: ¹H NMR (300 MHz, $CDCl_3$) δ : 1.41 (3H, t, *J* = 7.1 Hz), 2.42–2.64 (4H, m), 2.90 (2H, d, *J* = 5.2 Hz), 3.80 (3H, s), 3.84 (3H, s), 3.80–3.88 (1H, m), 4.02 (2H, q, *J* = 7.1 Hz), 4.08–4.13 (1H, m), 5.66 (1H, br), 6.46–6.75 (4H, m), 6.81 (1H, d, *J* = 8.0 Hz); ¹³C NMR (75 MHz, $CDCl_3$) δ : 14.85, 30.94, 34.48, 38.15, 40.90, 46.58, 55.85, 64.38, 71.24, 111.11, 111.61, 112.29, 113.94, 120.43, 121.83, 129.20, 130.30, 144.47, 145.80, 147.62, 148.81, 178.51; IR (neat): 1516 (C=C), 1766 (C=O), 3446 (OH) cm^{-1} ; MS (EI) *m/z* 386 (M^+); HRMS (EI): calcd for $C_{22}H_{26}O_6$: 386.1729 (M^+), found: 386.1724; $[\alpha]_D^{25}$ –20.5 (c 0.98, $CHCl_3$).

4.1.2.3. (3*R*,4*R*)-4-(3,4-Dimethoxybenzyl)-3-(4-hydroxy-3-propoxybenzyl)dihydrofuran-2-one (4b**).** By the procedure similar to synthesis of **4a**, (–)-arctigenin derivative **4b** was prepared from **3** and *n*-PrBr (18% in 2 steps) as a colorless oil: ¹H NMR (300 MHz, $CDCl_3$) δ : 1.04 (3H, t, *J* = 1.9 Hz), 1.77–1.87 (2H, m), 2.42–2.67 (4H, m), 2.81–3.01 (2H, m), 3.78–3.86 (7H, m), 3.90–4.00 (2H, m), 4.09–4.14 (1H, m), 5.59–5.63 (1H, br), 6.47–6.85 (6H, m); ¹³C NMR (75 MHz, $CDCl_3$) δ : 10.60, 22.60, 29.34, 31.81, 34.55, 38.22, 41.49, 46.65, 53.80, 55.82, 70.35, 71.29, 111.71, 113.94, 115.27, 120.47, 121.85, 112.34, 129.28,

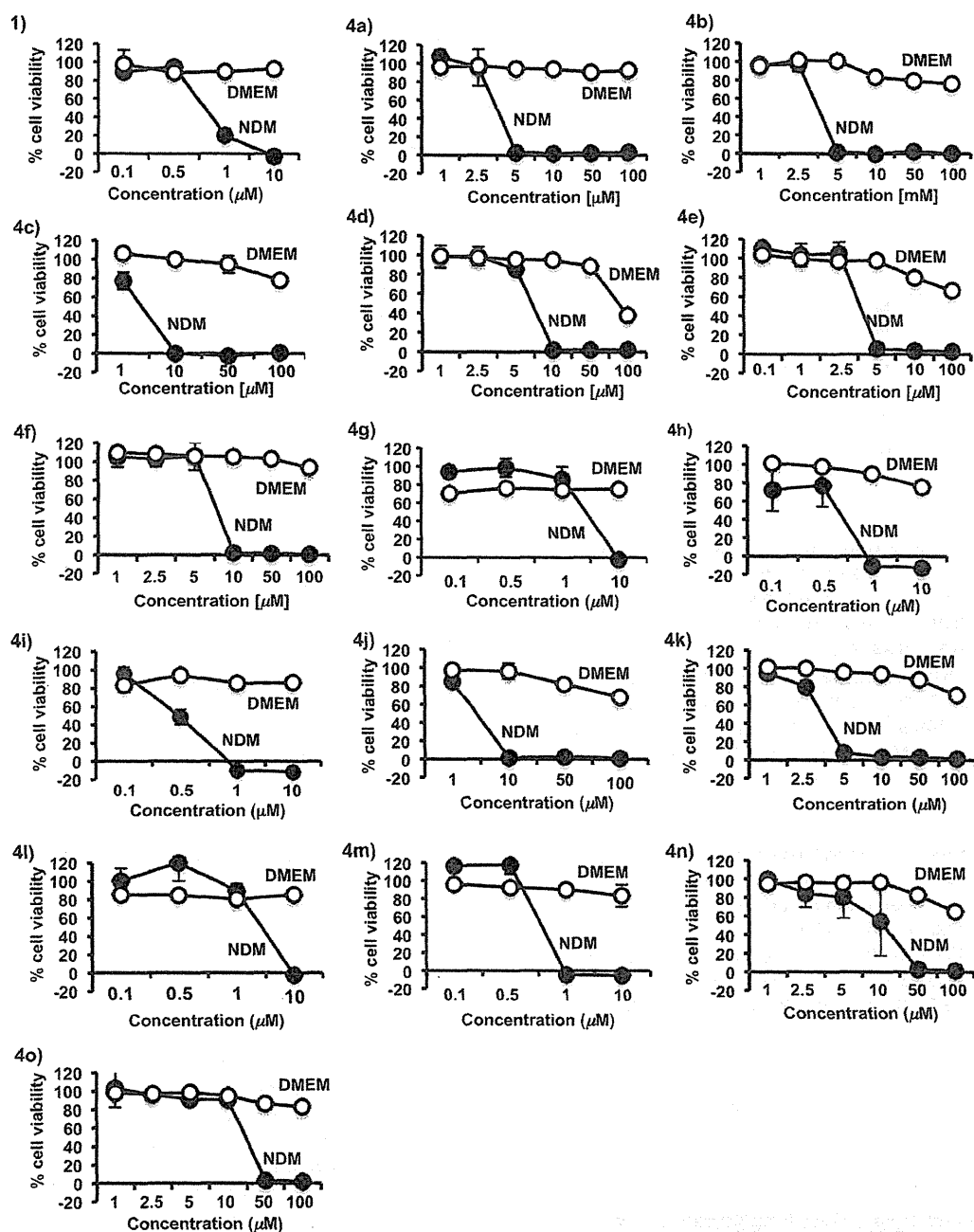


Fig. 2. Effects of (–)-arctigenin derivatives on cell survival in the PANC-1 cell line under nutrient-deprived conditions. Cells were seeded at a density of 2×10^4 per well in 96-well plates and incubated in fresh complete medium for 24 h. The cells were then washed with PBS and the medium was changed to nutrient-deprived medium (NDM, ●) or normal DMEM (○) together containing graded concentrations of (–)-arctigenin derivatives. Points, mean from triplicate experiments. The cell number at the start of the starvation was considered to be 100%. The cell count was measured by the WST-8 cell counting kit method, as described in experimental. The numbers 1 and 4a–o mean the data of (–)-arctigenin (1) and (–)-arctigenin derivatives 4a–o, respectively.

130.59, 144.52, 147.69, 178.54; IR (neat): 1456 (C=C), 1769 (C=O) cm^{-1} ; MS (EI) m/z 400 (M^+); HRMS (EI): calcd for $C_{23}H_{28}O_6$: 400.1886 (M^+), found: 400.1893; $[\alpha]_D^{25}$ –15.7 (c 1.45, CHCl_3).

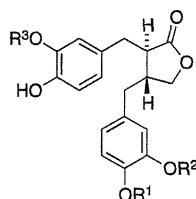
4.1.2.4. (3R,4R)-4-(3,4-Dimethoxybenzyl)-3-(4-hydroxy-3-*i*-propoxybenzyl)dihydrofuran-2-one (4c). By the procedure similar to synthesis of 4a, (–)-arctigenin derivative 4c was prepared from 3 and *i*-PrI (18% in 2 steps) as a pale yellow oil: ^1H NMR (300 MHz, CDCl_3) δ : 1.31–1.35 (6H, m), 1.59 (1H, br), 2.41–2.68 (4H, m), 2.80–3.00 (2H, m), 3.80–3.88 (7H, m), 4.07–4.12 (1H, m), 4.49–4.57 (1H,

m), 6.48–6.84 (6H, m); ^{13}C NMR (75 MHz, CDCl_3) δ : 22.02, 34.39, 3.12, 41.45, 46.65, 55.81, 71.19, 111.25, 111.68, 113.41, 114.18, 115.49, 120.61, 122.09, 129.26, 130.43, 144.70, 145.48, 146.59, 147.84, 149.02, 178.72; IR (neat): 1716 (C=O), 3629 (OH) cm^{-1} ; MS (EI) m/z 400 (M^+); HRMS (EI): calcd for $C_{23}H_{28}O_6$: 400.1886 (M^+), found: 400.1926; $[\alpha]_D^{24}$ –37.7 (c 0.41, CHCl_3).

4.1.2.5. (3R,4R)-4-(3,4-Dimethoxybenzyl)-3-(4-hydroxy-3-butyloxybenzyl)dihydrofuran-2-one (4d). By the procedure similar to synthesis of 4a, (–)-arctigenin derivative 4d was prepared from 3

Table 1

Preferential cytotoxicity of (–)-arctigenin (**1**) and series of new (–)-arctigenin derivatives **4a–4o** against human pancreatic cancer PANC-1 cells in nutrient-deprived medium (NDM).



Compound	R ¹	R ²	R ³	PC ₅₀ (μM)	Compound	R ¹	R ²	R ³	PC ₅₀ (μM)
1 (arctigenin)	Me	Me	Me	0.80	4h	Me	Et	Et	0.66
4a	Me	Me	Et	3.74	4i	Et	Me	Me	0.49
4b	Me	Me	<i>n</i> -Pr	3.74	4j	Et	Me	Et	4.77
4c	Me	Me	<i>i</i> -Pr	4.16	4k	Me	Et	<i>n</i> -Pr	3.54
4d	Me	Me	<i>n</i> -Bu	7.14	4l	Et	Et	Me	4.85
4e	Me	Me	<i>n</i> -Hex	3.89	4m	Et	Et	Et	0.78
4f	Me	Me	HO(CH ₂) ₂	7.70	4n	Me	<i>n</i> -Pr	<i>n</i> -Pr	13.6
4g	Me	Et	Me	4.71	4o	Et	<i>n</i> -Pr	<i>n</i> -Pr	28.6

and *n*-BuBr (25% in 2 steps) as a colorless oil: ¹H NMR (300 MHz, CDCl₃) δ: 0.98 (3H, t, *J* = 7.1 Hz), 1.48 (2H, dd, *J* = 15.1, 7.1 Hz), 1.74–1.83 (2H, m), 2.41–2.66 (4H, m), 2.80–3.02 (2H, m), 3.82 (3H, s), 3.83 (3H, s), 3.85 (1H, m), 3.94–4.03 (2H, m), 4.08–4.14 (1H, m), 5.59 (1H, m), 6.50–6.84 (6H, m); ¹³C NMR (75 MHz, CDCl₃) δ: 13.97, 19.32, 31.31, 55.82, 55.92, 68.60, 68.65, 71.21, 71.27, 111.19, 111.67, 112.32, 113.92, 120.46, 129.29, 130.34, 130.46, 144.52, 144.71, 145.59, 145.96, 147.69, 148.92, 178.53; IR (neat): 1515 (C=C), 1769 (C=O), 3446 (OH) cm^{−1}; MS (EI) *m/z* 414 (M⁺); HRMS (EI): calcd for C₂₄H₃₀O₆: 414.2042 (M⁺), found: 414.2000; [α]_D²⁶ −20.2 (c 1.15, CHCl₃).

4.1.2.6. (3*R*,4*R*)-4-(3,4-Dimethoxybenzyl)-3-(3-hexyloxy-4-hydroxybenzyl)dihydrofuran-2-one (4e). By the procedure similar to synthesis of **4a**, (–)-arctigenin derivative **4e** was prepared from **3** and 1-bromohexane (35% in 2 steps) as a pale yellow oil: ¹H NMR (300 MHz, CDCl₃) δ: 0.90 (3H, t, *J* = 6.4 Hz), 1.25–1.27 (2H, m), 1.33–1.35 (4H, m), 1.45 (2H, m), 1.75–2.66 (4H, m), 2.81–3.01 (2H, m), 3.82 (3H, s), 3.85 (3H, s), 3.84–3.89 (1H, m), 3.94–4.02 (2H, m), 4.09–4.14 (1H, m), 5.56–5.61 (1H, m), 6.47–6.84 (6H, m); ¹³C NMR (75 MHz, CDCl₃) δ: 14.11, 22.67, 25.78, 29.25, 31.62, 34.56, 38.22, 40.02, 46.65, 55.82, 68.92, 71.21, 111.19, 111.67, 112.32, 113.92, 115.25, 120.56, 121.83, 129.29, 130.43, 130.34, 144.52, 147.67, 148.92, 178.53;

IR (neat): 1457 (C=C), 1764 (C=O), 3689 (OH) cm^{−1}; MS (EI) *m/z* 442 (M⁺); HRMS (EI): calcd for C₂₆H₃₄O₆: 442.2355 (M⁺), found: 442.2336; [α]_D²⁶ −10.1 (c 0.65, CHCl₃).

4.1.2.7. (3*R*,4*R*)-4-(3,4-Dimethoxybenzyl)-3-[4-hydroxy-3-(2-hydroxyethoxy)benzyl]dihydrofuran-2-one (4f). By the procedure similar to synthesis of **4a**, (–)-arctigenin derivative **4f** was prepared from **3** and 2-benzyloxyethanol (20% in 2 steps) as a colorless oil: ¹H NMR (300 MHz, CDCl₃) δ: 2.42–2.59 (4H, m), 2.78–2.94 (2H, m), 3.76 (3H, s), 3.83 (3H, s), 3.73–3.80 (1H, m), 3.86–4.07 (6H, m), 4.13–4.16 (1H, m), 6.40–6.75 (4H, m), 6.81 (1H, d, *J* = 8.0 Hz); ¹³C NMR (75 MHz, CDCl₃) δ: 28.24, 38.22, 40.69, 46.53, 55.72, 55.97, 61.08, 69.82, 71.45, 111.30, 111.56, 113.00, 115.02, 120.67, 122.55, 129.00, 130.44, 145.02, 146.10, 147.38, 148.72, 178.83; IR (neat): 1517 (C=C), 1765 (C=O), 3420 (OH) cm^{−1}; MS (EI) *m/z* 402 (M⁺); HRMS (EI): calcd for C₂₃H₂₈O₆: 402.1679 (M⁺), found: 402.1671; [α]_D²⁶ −19.7 (c 1.10, CHCl₃).

4.1.3. Synthesis of (–)-arctigenin derivatives **4g–4o**

4.1.3.1. (4-Benzyloxy-3-methoxymethoxyphenyl)methanol (7). To a stirred solution of 4-benzyloxy-3-methoxymethoxybenzaldehyde (**6**) [14] (7.03 g, 25.8 mmol) in MeOH (50 mL) was added NaBH₄ (3.88 g, 103 mmol) at 0 °C, and the resulting mixture was stirred at room temperature for 2 h. The reaction was quenched with H₂O (50 mL), and the aqueous mixture was extracted with CH₂Cl₂ (50 mL × 3). The organic extracts were combined, dried over MgSO₄. The solvent was removed under reduced pressure, and the residue was chromatographed on silica gel (40 g, hexane:acetone = 3:1) to give **7** (6.66 g, 95%) as a pale yellow oil: ¹H NMR (300 MHz, CDCl₃) δ: 1.26 (1H, br), 3.53 (3H, s), 5.01 (2H, s), 5.16 (2H, s), 5.24 (2H, s), 6.88–6.96 (2H, m), 7.16 (1H, d, *J* = 1.9 Hz), 7.30–7.45 (5H, m); ¹³C NMR (75 MHz, CDCl₃) δ: 56.13, 64.64, 70.88, 95.40, 114.25, 116.22, 121.06, 126.98, 127.61, 128.27, 134.16, 136.82, 146.60, 148.19; IR (neat): 1511 (C=C), 3419 (OH) cm^{−1}; MS (EI) *m/z* 274 (M⁺); HRMS (EI): calcd for C₁₆H₁₈O₄: 274.1205 (M⁺), found: 274.1188.

4.1.3.2. 2-(4-Benzyloxy-3-methoxymethoxybenzyl)malonic acid diethyl ester (8). To a stirred solution of **7** (711 mg, 2.59 mmol) in CH₂Cl₂ (26 mL) were added NEt₃ (0.43 mL, 3.11 mmol) and MsCl (0.22 mL, 2.85 mmol) at 0 °C, and the reaction mixture was stirred at room temperature for 0.5 h. The reaction was quenched with sat. NaHCO₃ (aq) (20 mL), and the organic layer was separated. The aqueous layer was extracted with CH₂Cl₂ (30 mL × 3), and the organic layer and extracts were combined, dried over MgSO₄. The

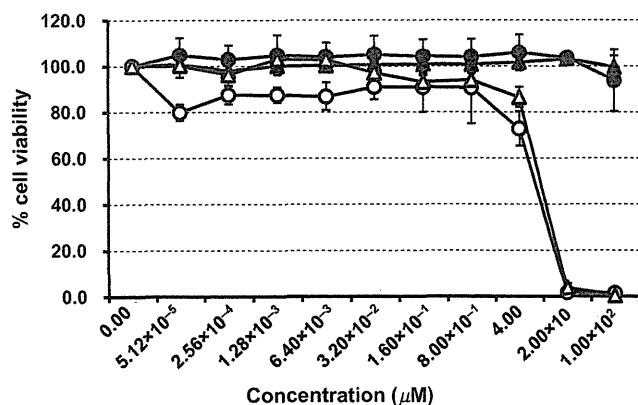


Fig. 3. Effect of triethoxy derivative **4m** and (–)-arctigenin (**1**) on cell survival in the CAPAN-1 cell line under glucose-deprived conditions. ●, (–)-arctigenin (**1**) in normal DMEM; ▲, triethoxy derivative **4m** in normal DMEM; ○, (–)-arctigenin (**1**) in glucose-deprived medium; △, triethoxy derivative **4m** in glucose-deprived medium.

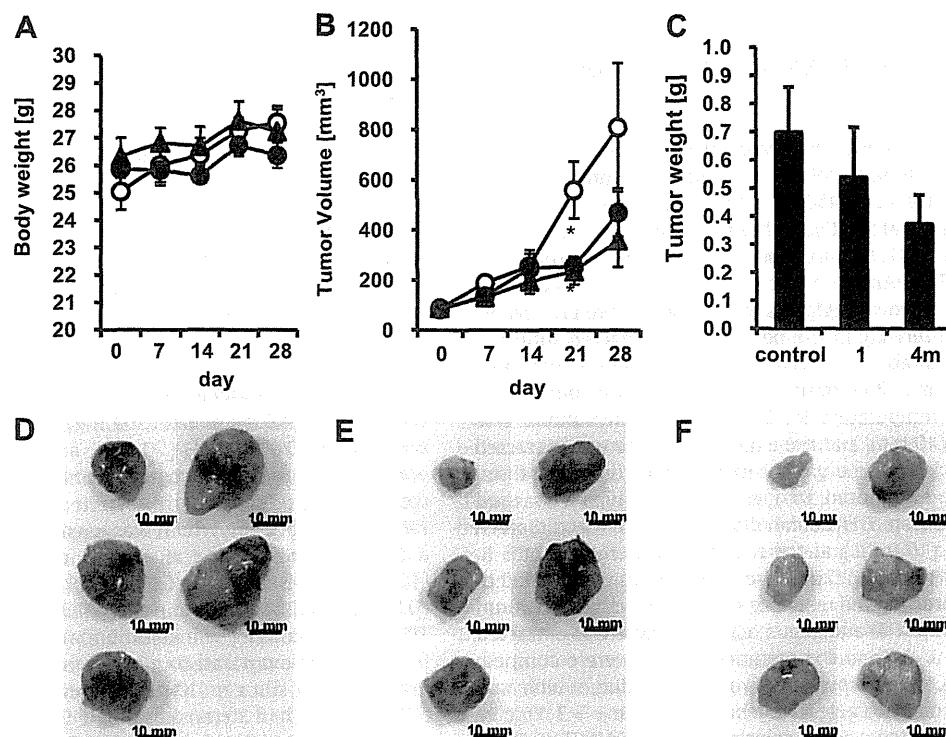


Fig. 4. Effect of triethoxy derivative **4m** and (–)-arctigenin (**1**) on the growth of CAPAN-1 cells in nude mice. A, body weight of mice. ○, control group ($n = 5$); ●, group treated with triethoxy derivative **4m** ($n = 6$); ▲, group treated with (–)-arctigenin (**1**) ($n = 5$). B, the tumor volume in the mice. ○, control group; ●, group treated with triethoxy derivative **4m**; ▲, group treated with (–)-arctigenin (**1**). C, wet weight of the tumor in the mice on the last day of the experiment. D–F, photographs of the tumor after sacrifice on the last day of control group, of group treated with (–)-arctigenin (**1**), and of group treated with triethoxy derivative **4m**, respectively.

solvent was removed under reduced pressure to give a pale yellow oil, which was used directly in the next step. To a stirred solution of diethyl malonate (0.79 mL, 5.18 mmol) in DMF (10 mL) was added NaH (60%, 207 mg, 5.18 mmol) at 0 °C, and the resulting mixture was stirred at room temperature for 1 h. To the solution was added a solution of the oil obtained above in DMF (2 mL) at 0 °C, and the reaction mixture was stirred at room temperature for 20 h. The reaction was quenched with sat. NaHCO_3 (aq) (10 mL), and the aqueous mixture was extracted with Et_2O (20 mL \times 3). The organic extracts were combined, dried over MgSO_4 , evaporated to give a pale yellow oil which was chromatographed on silica gel (20 g, hexane:acetone = 15:1) to give **8** (776 mg, 72% in 2 steps) as a pale yellow oil: ^1H NMR (300 MHz, CDCl_3) δ : 1.22 (6H, t, $J = 7.1$ Hz), 3.13 (2H, d, $J = 7.6$ Hz), 3.50 (3H, s), 3.60 (1H, t, $J = 7.6$ Hz), 4.16 (4H, q, $J = 7.1$ Hz), 5.11 (2H, s), 5.19 (2H, s), 6.74–6.83 (2H, m), 7.00 (1H, d, $J = 1.7$ Hz), 7.28–7.42 (5H, m); ^{13}C NMR (75 MHz, CDCl_3) δ : 14.05, 34.09, 53.93, 56.16, 61.35, 70.92, 95.64, 114.31, 117.98, 122.74, 127.01, 127.63, 128.31, 130.09, 136.95, 146.64, 147.71, 168.56; IR (neat): 1510 ($\text{C}=\text{C}$), 1732 ($\text{C}=\text{O}$) cm^{-1} ; MS (EI) m/z 416 (M^+); HRMS (EI): calcd for $\text{C}_{23}\text{H}_{28}\text{O}_7$: 416.1835 (M^+), found: 416.1832.

4.1.3.3. (R)-Acetic acid 3-(4-benzyloxy-3-methoxymethoxyphenyl)-2-hydroxymethylpropyl ester ((+)-9**).** To a stirred solution of **8** (1.66 g, 3.98 mmol) in THF (40 mL) was added LiAlH_4 (378 mg, 9.96 mmol) at 0 °C, and the resulting suspension was refluxed for 12 h. The reaction was quenched with 10% NaOH (aq) (20 mL), and the mixture was extracted with AcOEt (20 mL \times 5). The organic extracts were combined, dried over MgSO_4 , and the solvent was evaporated to give diol, which was used directly in the next step. To a stirred solution of the diol obtained above in $i\text{-Pr}_2\text{O}$ –THF (20 mL, 4:1) were added lipase-PS (397 mg) and vinyl acetate (0.52 mL,

5.67 mmol), and the reaction mixture was stirred at room temperature for 2 h. The catalyst was filtered and the filtrate was evaporated to give residue, which was chromatographed on silica gel (30 g, hexane:acetone = 15:1) to give (+)-**9** (1.20 g, 80% in 2 steps) as a pale yellow oil. The enantiomeric excess of (+)-**9** was determined to be a 98% ee by the following HPLC analysis; chiralcel OJ (0.46 cm \times 25 cm), hexane/2-propanol = 1/1, flow rate = 0.5 mL/min, $\lambda = 254$ nm, (+)-**9**; $t_R = 29.7$ min, (–)-**9**; 25.5 min ^1H NMR (300 MHz, CDCl_3) δ : 1.70 (1H, br), 2.09 (3H, s), 2.17 (1H, s), 2.55–2.62 (2H, m), 3.47–3.62 (2H, m), 3.52 (3H, s), 4.03–4.20 (2H, m), 5.13 (2H, s), 5.21 (2H, s), 6.72–6.98 (3H, m), 7.30–7.44 (5H, m); ^{13}C NMR (75 MHz, CDCl_3) δ : 20.99, 33.75, 42.47, 56.27, 62.08, 63.94, 71.14, 95.72, 114.534, 118.21, 122.92, 127.11, 127.71, 128.40, 132.46, 137.11, 146.82, 147.48, 171.47; IR (neat): 1739 ($\text{C}=\text{O}$), 3165 (OH) cm^{-1} ; MS (EI) m/z 374 (M^+); HRMS (EI): calcd for $\text{C}_{21}\text{H}_{26}\text{O}_6$: 374.1729 (M^+), found: 374.1723; $[\alpha]_D^{26} +13.5$ (c 1.14, CHCl_3).

4.1.3.4. (R)-Acetic acid 3-(4-benzyloxy-3-methoxymethoxyphenyl)-2-methanesulfonyloxymethylpropyl ester (10**).** To a stirred solution of (+)-**9** (666 mg, 1.78 mmol) in CH_2Cl_2 (8 mL) were added MsCl (0.15 mL, 1.95 mmol) and NEt_3 (0.32 mL, 2.31 mmol) at 0 °C, and the reaction mixture was stirred at room temperature for 0.5 h. The reaction was quenched with H_2O (8 mL), and the aqueous mixture was extracted with CH_2Cl_2 (10 mL \times 3). The organic extracts were combined, dried over MgSO_4 , and evaporated. The residue was chromatographed on silica gel (30 g, hexane:acetone = 15:1) to give **10** (775 mg, 96%) as a pale yellow oil: ^1H NMR (300 MHz, CDCl_3) δ : 2.03 (3H, s), 2.27–2.34 (1H, m), 2.61 (2H, d, $J = 7.42$ Hz), 2.93 (3H, s), 3.47 (3H, s), 3.96–4.19 (4H, m), 5.08 (2H, s), 5.18 (2H, s), 6.69–6.95 (3H, m), 7.24–7.41 (5H, m); ^{13}C NMR (75 MHz, CDCl_3) δ : 20.91, 33.41, 37.26, 39.61, 56.29, 62.94, 68.34, 71.13, 95.67, 114.65, 118.05,

122.84, 127.12, 127.76, 128.42, 130.88, 136.98, 146.98, 147.72, 170.56; IR (KBr): 1242 (S=O), 1736 (C=O) cm^{-1} ; MS (EI) m/z 452 (M^+); HRMS (EI): calcd for $\text{C}_{22}\text{H}_{28}\text{O}_8$: 452.1505 (M^+), found: 452.1512; $[\alpha]_{\text{D}}^{25} +2.76$ (c 1.40, CHCl_3).

4.1.3.5. (R)-4-(4-Benzyloxy-3-hydroxybenzyl)dihydrofuran-2-one (11). To a stirred solution of **10** (993 mg, 2.19 mmol) in DMSO (20 mL) was added KCN (150 mg, 2.19 mmol), and the resulting mixture was heated at 90 °C for 3 h. After cooling, the reaction was quenched with H_2O (20 mL), and the aqueous mixture was extracted with $\text{Et}_2\text{O}/\text{AcOEt}$ (1:1, 20 mL \times 3). The organic extracts were combined, dried over MgSO_4 , and evaporated to give cyanide, which was used directly in the next step. To a stirred solution of cyanide obtained above in $\text{THF}-\text{H}_2\text{O}$ (3:1, 8 mL) was added $\text{LiOH}\cdot\text{H}_2\text{O}$ (91.9 mg, 2.19 mmol), and the reaction mixture was stirred at room temperature for 24 h. The reaction mixture was diluted with H_2O (10 mL), and the aqueous mixture was extracted with Et_2O (20 mL \times 3). The organic extracts were combined, dried over MgSO_4 , and evaporated to give alcohol, which was used directly in the next step. The alcohol obtained above was dissolved in 10% NaOH (aq) (10 mL), and the mixture was refluxed for 5 h. After cooling, 10% HCl (aq) (20 mL) and THF (20 mL) were added to the reaction mixture, and the resulting solution was stirred at room temperature for 50 h. The aqueous reaction mixture was extracted with Et_2O (30 mL \times 3), and the organic extracts were combined, dried over MgSO_4 , and evaporated to give a residue, which was chromatographed on silica gel (20 g, hexane:acetone = 3:1) to give **11** (479 mg, 73% in 4 steps) as a colorless solid: ^1H NMR (300 MHz, CDCl_3) δ : 2.17–2.32 (1H, m), 2.52–2.69 (3H, m), 2.74–2.86 (1H, m), 3.91–4.05 (1H, m), 4.30–4.36 (1H, m), 5.09 (2H, s), 5.67 (1H, br), 6.59–6.89 (3H, m), 7.36–7.85 (5H, m); ^{13}C NMR (75 MHz, CDCl_3) δ : 34.25, 37.22, 38.41, 71.22, 72.63, 112.26, 114.78, 120.04, 127.69, 128.32, 128.61, 131.72, 136.09, 144.50, 145.89, 176.68; IR (KBr): 1647 (C=O), 3445 (OH) cm^{-1} ; MS (EI) m/z 298 (M^+); HRMS (EI): calcd for $\text{C}_{18}\text{H}_{18}\text{O}_4$: 298.1205 (M^+), found: 298.1204; $[\alpha]_{\text{D}}^{26} +5.6$ (c 0.13, CHCl_3); mp: 137–139 °C.

4.1.3.6. (R)-4-(4-Benzyloxy-3-methoxybenzyl)dihydrofuran-2-one (12a). To a stirred solution of **11** (330 mg, 1.1 mmol) in acetone (15 mL) were added K_2CO_3 (168 mg, 1.2 mmol) and MeI (0.41 mL, 6.6 mmol), and the reaction mixture was refluxed for 24 h. After cooling, the insoluble materials were filtered, and the filtrate was evaporated to give a residue, which was chromatographed on silica gel (15 g, hexane:acetone = 4:1) to give **12a** (304 mg, 88%) as a colorless oil: ^1H NMR (300 MHz, CDCl_3) δ : 2.17 (2H, s), 2.24–2.30 (1H, m), 3.88 (3H, s), 4.03–4.05 (1H, m), 4.30–4.35 (1H, m), 5.13 (2H, s), 6.61–6.64 (2H, m), 6.81–6.83 (1H, m), 7.27–7.45 (5H, m); ^{13}C NMR (75 MHz, CDCl_3) δ : 34.29, 37.30, 38.64, 56.06, 71.11, 72.60, 112.32, 114.23, 120.52, 127.12, 127.72, 128.40, 131.25, 136.96, 146.91, 149.66, 176.65; IR (neat): 1654 (C=C), 1774 (C=O) cm^{-1} ; MS (EI) m/z 312 (M^+); HRMS (EI): calcd for $\text{C}_{19}\text{H}_{20}\text{O}_4$: 312.1362 (M^+), found: 312.1380; $[\alpha]_{\text{D}}^{25} +4.9$ (c 0.95, CHCl_3).

4.1.3.7. (R)-4-(4-Benzyloxy-3-ethoxybenzyl)dihydrofuran-2-one (12b). By the procedure similar to preparation of **12a**, **12b** was prepared from **11** and EtI (84%) as a pale yellow oil: ^1H NMR (300 MHz, CDCl_3) δ : 1.44 (3H, t, $J = 4.4$ Hz), 2.28 (1H, dd, $J = 17.3$, 6.9 Hz), 2.60 (1H, dd, $J = 17.3$, 8.0 Hz), 2.67–2.84 (3H, m), 4.02–4.13 (3H, m), 4.32 (1H, dd, $J = 9.1$, 6.9 Hz), 5.12 (2H, s), 6.60–6.69 (2H, m), 6.84 (1H, d, $J = 8.2$ Hz), 7.30–7.77 (5H, m); ^{13}C NMR (75 MHz, CDCl_3) δ : 15.03, 34.29, 37.31, 38.61, 64.74, 71.37, 72.62, 114.29, 115.22, 120.73, 127.08, 127.63, 128.34, 131.46, 137.20, 147.33, 149.18, 176.67; IR (neat): 1507 (C=C), 1772 cm^{-1} (C=O); MS (EI) m/z 326 (M^+); HRMS (EI): calcd for $\text{C}_{20}\text{H}_{22}\text{O}_4$: 326.1518 (M^+), found: 326.1523; $[\alpha]_{\text{D}}^{26} +3.4$ (c 1.78, CHCl_3).

4.1.3.8. (R)-4-(4-Benzyloxy-3-propoxybenzyl)dihydrofuran-2-one (12c). By the procedure similar to preparation of **12a**, **12c** was prepared from **11** and $n\text{-PrBr}$ (87%) as a colorless oil: ^1H NMR (600 MHz, CDCl_3) δ : 1.04 (3H, t, $J = 7.0$ Hz), 1.84 (2H, sextet, $J = 7.0$ Hz), 2.26 (1H, dd, $J = 17.5$, 7.0 Hz), 2.57 (1H, dd, $J = 17.5$, 8.1 Hz), 2.64–2.71 (2H, m), 2.74–2.83 (1H, m), 3.96 (2H, t, $J = 7.0$ Hz), 4.00 (1H, dd, $J = 9.2$, 5.9 Hz), 4.30 (1H, dd, $J = 9.2$, 7.0 Hz), 5.09 (2H, s), 6.60 (1H, d, $J = 8.1$ Hz), 6.67 (1H, s), 6.82 (1H, d, $J = 8.1$ Hz), 7.27–7.42 (5H, m); ^{13}C NMR (100 MHz, CDCl_3) δ : 10.46, 22.55, 34.07, 37.15, 38.43, 70.65, 71.32, 72.55, 114.28, 115.38, 120.69, 127.10, 127.63, 128.34, 131.61, 137.31, 147.37, 149.52, 176.84; IR (neat): 1508 (C=C), 1773 (C=O) cm^{-1} ; MS (EI) m/z 340 (M^+); HRMS (EI): calcd for 340.1675 (M^+), found: 340.1667; $[\alpha]_{\text{D}}^{26} -1.0$ (c 1.05, CHCl_3).

4.1.3.9. (R)-4-(3,4-Dimethoxybenzyl)dihydrofuran-2-one (13a). To a stirred solution of **12a** (302 mg, 0.97 mmol) in MeOH (5 mL) was added 20% $\text{Pd}(\text{OH})_2$ (20 mg), and the resulting suspension was stirred under a hydrogen atmosphere at 1 atm for 15 h. The catalyst was removed by filtration and the filtrate was evaporated to give phenol, which was used directly in the next step. To a stirred solution of the phenol obtained above in acetone (10 mL) were added K_2CO_3 (201.1 mg, 1.46 mmol) and MeI (0.18 mL, 2.92 mmol), and the resulting mixture was refluxed for 19 h. After cooling, the insoluble materials were filtered, and the filtrate was evaporated to give a residue, which was chromatographed on silica gel (10 g, hexane:acetone = 4:1) to give **13a** (130 mg, 55% in 2 steps) as a pale yellow oil: ^1H NMR (300 MHz, CDCl_3) δ : 2.33 (1H, dd, $J = 18.0$, 9.3 Hz), 2.61 (1H, dd, $J = 17.4$, 8.1 Hz), 2.70–2.87 (3H, m), 3.87 (3H, s), 3.88 (3H, s), 4.05 (1H, dd, $J = 9.3$, 6.3 Hz), 4.33 (1H, dd, $J = 9.3$, 6.6 Hz), 6.66–6.72 (2H, m), 6.82 (1H, d, $J = 8.1$ Hz); $[\alpha]_{\text{D}}^{25} +22.2$ (c 0.87, CHCl_3) (ref. [19], $[\alpha]_{\text{D}}^{25} +23.8$).

4.1.3.10. (R)-4-(4-Ethoxy-3-methoxybenzyl)dihydrofuran-2-one (13b). By the procedure similar to preparation of **13a**, **13b** was prepared from **12a** and EtI (55% in 2 steps) as a pale yellow oil: ^1H NMR (300 MHz, CDCl_3) δ : 1.46 (3H, t, $J = 7.1$ Hz), 2.29 (1H, dd, $J = 17.6$, 6.9 Hz), 2.63 (1H, dd, $J = 17.6$, 8.0 Hz), 2.71–2.88 (3H, m), 3.86 (3H, s), 4.03 (1H, dd, $J = 9.1$, 6.9 Hz), 4.06 (2H, q, $J = 7.1$ Hz), 4.34 (1H, dd, $J = 9.1$, 6.9 Hz), 6.65–6.68 (2H, m), 6.81 (1H, d, $J = 8.2$ Hz); ^{13}C NMR (75 MHz, CDCl_3) δ : 14.92, 34.32, 37.36, 38.65, 55.98, 64.38, 72.63, 112.01, 112.84, 120.56, 130.59, 147.06, 149.26, 176.68; IR (neat): 1514 (C=C), 1778 (C=O) cm^{-1} ; MS (EI) m/z 250 (M^+); HRMS (EI): calcd for $\text{C}_{14}\text{H}_{18}\text{O}_4$: 250.1205 (M^+), found: 250.1192; $[\alpha]_{\text{D}}^{24} +4.4$ (c 1.66, CHCl_3).

4.1.3.11. (R)-4-(3-Ethoxy-4-methoxybenzyl)dihydrofuran-2-one (13c). By the procedure similar to preparation of **13a**, **13c** was prepared from **12b** and MeI (55% in 2 steps) as a pale yellow oil: ^1H NMR (300 MHz, CDCl_3) δ : 1.47 (3H, t, $J = 6.9$ Hz), 2.29 (1H, dd, $J = 17.3$, 6.6 Hz), 2.61 (1H, dd, $J = 17.3$, 8.0 Hz), 2.67–2.87 (3H, m), 3.86 (3H, s), 4.01–4.12 (3H, m), 4.34 (1H, dd, $J = 9.1$, 6.6 Hz), 6.62–6.69 (2H, m), 6.81 (1H, d, $J = 8.0$ Hz); ^{13}C NMR (75 MHz, CDCl_3) δ : 14.87, 34.24, 37.31, 38.54, 55.95, 64.35, 72.58, 111.61, 113.24, 120.54, 130.52, 148.01, 148.22, 176.63; IR (neat): 1541 (C=C), 1771 (C=O) cm^{-1} ; MS (EI) m/z 250 (M^+); HRMS (EI): calcd for $\text{C}_{14}\text{H}_{18}\text{O}_4$: 250.1205 (M^+), found: 250.1207; $[\alpha]_{\text{D}}^{27} +4.4$ (c 1.94, CHCl_3).

4.1.3.12. (R)-4-(3,4-Diethoxybenzyl)dihydrofuran-2-one (13d). By the procedure similar to preparation of **13a**, **13d** was prepared from **12b** and EtI (47% in 2 steps) as a pale yellow oil: ^1H NMR (300 MHz, CDCl_3) δ : 1.41–1.47 (6H, m), 2.28 (1H, dd, $J = 17.3$, 6.6 Hz), 2.59 (1H, dd, $J = 17.3$, 8.0 Hz), 2.67–2.86 (3H, m), 4.00–4.11 (5H, m), 4.32 (1H, dd, $J = 9.3$, 6.6 Hz), 6.64–6.67 (2H, m), 6.81 (1H, d, $J = 8.5$ Hz); ^{13}C NMR (75 MHz, CDCl_3) δ : 14.97, 34.30, 37.36, 38.61, 64.64, 64.69, 72.65,

113.70, 114.12, 120.78, 130.70, 147.53, 148.72, 176.68; IR (neat): 1507 (C=C), 1771 (C=O) cm^{-1} ; MS (EI) m/z 264 (M^+); HRMS (EI): calcd for $\text{C}_{15}\text{H}_{20}\text{O}_4$: 264.1362 (M^+), found: 264.1369; $[\alpha]_{\text{D}}^{26} +5.4$ (c 1.29, CHCl_3).

4.1.3.13. (R)-4-(4-Methoxy-3-propoxybenzyl)dihydrofuran-2-one (13e). By the procedure similar to preparation of **13a**, **13e** was prepared from **12c** and MeI (80% in 2 steps) as a pale yellow oil: ^1H NMR (400 MHz, CDCl_3) δ : 1.05 (3H, t, $J = 7.1$ Hz), 1.87 (2H, sextet, $J = 7.1$ Hz), 2.29 (1H, dd, $J = 17.5, 6.8$ Hz), 2.60 (1H, dd, $J = 17.5, 8.1$ Hz), 2.65–2.73 (2H, m), 2.77–2.84 (1H, m), 3.85 (1H, s), 3.96 (2H, t, $J = 7.1$ Hz), 4.03 (1H, dd, $J = 9.3, 6.1$ Hz), 4.33 (1H, dd, $J = 9.3, 7.0$ Hz), 6.67 (1H, s), 6.68 (1H, d, $J = 7.8$ Hz), 6.81 (1H, d, $J = 7.8$ Hz); ^{13}C NMR (100 MHz, CDCl_3) δ : 10.37, 22.44, 34.15, 37.23, 38.45, 56.00, 70.51, 72.57, 111.89, 113.52, 120.60, 130.67, 148.25, 148.62, 176.86; IR (neat): 1516 (C=C), 1778 (C=O) cm^{-1} ; MS (EI) m/z 264 (M^+); HRMS (EI): calcd for $\text{C}_{15}\text{H}_{20}\text{O}_4$: 264.1362 (M^+), found: 264.1345; $[\alpha]_{\text{D}}^{26} +3.2$ (c 1.05, CHCl_3).

4.1.3.14. (R)-4-(4-Ethoxy-3-propoxybenzyl)dihydrofuran-2-one (13f). By the procedure similar to preparation of **13a**, **13f** was prepared from **12c** and EtI (77% in 2 steps) as a pale yellow oil: ^1H NMR (400 MHz, CDCl_3) δ : 1.05 (3H, t, $J = 7.0$ Hz), 1.42 (3H, t, $J = 6.8$ Hz), 1.87 (2H, sextet, $J = 7.0$ Hz), 2.28 (1H, dd, $J = 17.5, 7.0$ Hz), 2.60 (1H, dd, $J = 17.5, 8.0$ Hz), 2.64–2.72 (2H, m), 2.74–2.85 (1H, m), 3.94 (2H, t, $J = 7.0$ Hz), 4.01–4.09 (3H, m), 4.32 (1H, dd, $J = 9.1, 6.9$ Hz), 6.64 (1H, s), 6.65 (1H, d, $J = 8.0$ Hz), 6.81 (1H, d, $J = 8.0$ Hz); ^{13}C NMR (100 MHz, CDCl_3) δ : 10.35, 14.79, 22.50, 34.10, 37.16, 38.38, 64.67, 70.72, 72.56, 114.05, 114.31, 120.78, 130.88, 147.64, 149.09, 176.85; IR (neat): 1510 (C=C), 1774 (C=O) cm^{-1} ; MS (EI) m/z 278 (M^+); HRMS (EI): calcd for $\text{C}_{16}\text{H}_{22}\text{O}_4$: 278.1518 (M^+), found: 278.1512; $[\alpha]_{\text{D}}^{26} +1.2$ (c 1.05, CHCl_3).

4.1.3.15. (3R,4R)-3-(4-Benzylloxy-3-methoxybenzyl)-4-(3-ethoxy-4-methoxybenzyl)dihydrofuran-2-one (14a). To a stirred solution of **13b** (29.6 mg, 0.12 mmol) in THF (2 mL) were added LiHMDS (1.6 M in THF, 0.12 mL, 0.18 mmol), HMPA (31 μL , 0.18 mmol) at -78°C , and the resulting solution was stirred at the same temperature for 0.5 h. To the reaction mixture was added a solution of 4-benzylloxy-3-methoxybenzyl bromide [20] (52.3 mg, 0.19 mmol) in THF (2 mL), and allowed to warm to room temperature over 1 h, and then stirred at the same temperature for 20 h. The reaction was quenched with H_2O (4 mL), and the aqueous mixture was extracted with Et_2O (10 mL \times 3). The organic extracts were combined, dried over MgSO_4 , and evaporated to give residue, which was chromatographed on silica gel (10 g, hexane:acetone = 4:1) to give **14a** (25 mg, 44%) as a pale yellow oil: ^1H NMR (300 MHz, CDCl_3) δ : 1.44 (3H, t, $J = 6.9$ Hz), 2.46–2.65 (4H, m), 2.91–2.95 (2H, m), 3.79–3.90 (1H, m), 3.84 (6H, s), 4.01 (2H, q, $J = 6.9$ Hz), 4.08–4.20 (1H, m), 5.12 (2H, s), 6.50–6.80 (6H, m), 7.28–7.43 (5H, m); ^{13}C NMR (75 MHz, CDCl_3) δ : 14.77, 34.48, 38.02, 41.09, 46.42, 55.90, 64.28, 65.18, 71.03, 71.16, 111.57, 112.85, 113.35, 113.92, 114.02, 120.54, 121.28, 127.17, 127.20, 127.76, 128.46, 130.32, 130.82, 137.06, 147.01, 148.09, 148.26, 149.73, 178.65; IR (neat): 1515 (C=C), 1770 (C=O) cm^{-1} ; MS (EI) m/z 476 (M^+); HRMS (EI): calcd for $\text{C}_{29}\text{H}_{32}\text{O}_6$: 476.2199 (M^+), found: 476.2197; $[\alpha]_{\text{D}}^{25} -16.4$ (c 0.77, CHCl_3).

4.1.3.16. (3R,4R)-3-(4-Benzylloxy-3-ethoxybenzyl)-4-(3-ethoxy-4-methoxybenzyl)dihydrofuran-2-one (14b). By the procedure similar to preparation of **14a**, **14b** was prepared from **13b** and 4-benzylloxy-3-ethoxybenzyl bromide [21] (59%) as a pale yellow oil: ^1H NMR (300 MHz, CDCl_3) δ : 1.34–1.40 (6H, m), 2.36–2.51 (4H, m), 2.81–2.85 (2H, m), 3.71–3.78 (1H, m), 3.75 (3H, s), 3.90–4.05 (5H, m), 5.02 (2H, s), 6.40–6.80 (6H, m), 7.14–7.35 (5H, m); ^{13}C NMR (75 MHz, CDCl_3) δ : 14.75, 14.82, 34.43, 37.99, 41.05, 46.39, 55.86, 64.22, 64.47, 71.14, 71.26, 111.51, 113.24, 114.59, 114.97, 120.51, 121.39, 127.11, 127.64, 128.35, 130.31, 130.99, 137.27, 147.33, 148.03, 148.23, 149.24, 178.65; IR (neat): 1507 (C=C), 1771 (C=O) cm^{-1} ;

MS (EI) m/z 490 (M^+); HRMS (EI): calcd for $\text{C}_{30}\text{H}_{34}\text{O}_6$: 490.2355 (M^+), found: 490.2383; $[\alpha]_{\text{D}}^{26} -14.8$ (c 1.46, CHCl_3).

4.1.3.17. (3R,4R)-3-(4-Benzylloxy-3-methoxybenzyl)-4-(4-ethoxy-3-methoxybenzyl)dihydrofuran-2-one (14c). By the procedure similar to preparation of **14a**, **14c** was prepared from **13c** and 4-benzylloxy-3-methoxybenzyl bromide [20] (43%) as a pale yellow oil: ^1H NMR (300 MHz, CDCl_3) δ : 1.45 (3H, t, $J = 6.9$ Hz), 2.47–2.63 (4H, m), 2.91–2.95 (2H, m), 3.84 (3H, s), 3.91 (3H, s), 3.91–3.95 (1H, m), 4.09 (2H, q, $J = 6.9$ Hz), 4.03–4.14 (1H, m), 5.16 (2H, s), 6.48–6.96 (6H, m), 7.28–7.45 (5H, m); ^{13}C NMR (75 MHz, CDCl_3) δ : 14.90, 34.58, 38.19, 41.13, 46.55, 55.98, 64.35, 65.29, 71.06, 110.88, 112.03, 112.82, 113.89, 113.97, 119.21, 120.44, 121.22, 127.69, 128.40, 130.26, 130.73, 134.03, 136.98, 146.91, 149.61, 178.49; IR (neat): 1261 (C=C), 1770 (C=O) cm^{-1} ; MS (EI) m/z 476 (M^+); HRMS (EI): calcd for $\text{C}_{29}\text{H}_{32}\text{O}_6$: 476.2199 (M^+), found: 476.2209; $[\alpha]_{\text{D}}^{26} -9.0$ (c 1.75, CHCl_3).

4.1.3.18. (3R,4R)-3-(4-Benzylloxy-3-ethoxybenzyl)-4-(4-ethoxy-3-methoxybenzyl)dihydrofuran-2-one (14d). By the procedure similar to preparation of **14a**, **14d** was prepared from **13c** and 4-benzylloxy-3-ethoxybenzyl bromide [21] (53%) as a pale yellow oil: ^1H NMR (300 MHz, CDCl_3) δ : 1.41–1.48 (6H, m), 2.44–2.67 (4H, m), 2.88–2.93 (2H, m), 3.79 (3H, s), 3.80–3.87 (1H, m), 4.02–4.14 (5H, m), 5.11 (2H, s), 6.45–6.96 (6H, m), 7.27–7.45 (5H, m); ^{13}C NMR (75 MHz, CDCl_3) δ : 14.62, 14.69, 30.69, 34.27, 37.89, 40.87, 46.28, 55.66, 64.12, 64.35, 71.04, 71.12, 111.92, 112.61, 114.52, 114.84, 120.38, 121.31, 127.02, 127.52, 128.23, 130.29, 130.91, 137.17, 146.91, 147.20, 149.10, 178.55; IR (neat): 1515 (C=C), 1771 (C=O) cm^{-1} ; MS (EI) m/z 490 (M^+); HRMS (EI): calcd for $\text{C}_{30}\text{H}_{34}\text{O}_6$: 490.2355 (M^+), found: 490.2383; $[\alpha]_{\text{D}}^{24} -17.9$ (c 1.14, CHCl_3).

4.1.3.19. (3R,4R)-3-(4-Benzylloxy-3-propoxybenzyl)-4-(3-ethoxy-4-methoxybenzyl)dihydrofuran-2-one (14e). By the procedure similar to preparation of **14a**, **14e** was prepared from **13b** and 4-benzylloxy-3-propoxybenzyl bromide, prepared from 4-benzyl-3-propoxybenzaldehyde [22], (40%) as a pale yellow oil: ^1H NMR (400 MHz, CDCl_3) δ : 1.05 (3H, t, $J = 7.1$ Hz), 1.45 (3H, t, $J = 7.8$ Hz), 1.84 (2H, sextet, $J = 7.1$ Hz), 2.46–2.64 (4H, m), 2.86–2.99 (2H, m), 3.80–3.87 (4H, m), 3.94 (2H, t, $J = 7.1$ Hz), 4.00 (2H, q, $J = 7.8$ Hz), 4.06–4.11 (1H, m), 5.10 (2H, s), 6.48–6.82 (6H, m), 7.28–7.44 (5H, m); ^{13}C NMR (100 MHz, CDCl_3) δ : 10.47, 14.75, 22.56, 34.47, 38.00, 41.10, 46.40, 55.87, 64.25, 70.53, 71.35, 111.55, 113.29, 114.71, 115.25, 120.52, 121.37, 127.18, 127.57, 127.63, 128.33, 130.35, 131.26, 137.34, 147.40, 148.07, 148.26, 149.57, 178.64; IR (neat): 1514 (C=C), 1771 (C=O) cm^{-1} ; MS (EI) m/z 504 (M^+); HRMS (EI): calcd for $\text{C}_{31}\text{H}_{36}\text{O}_6$: 504.2512 (M^+), found: 504.2538; $[\alpha]_{\text{D}}^{25} -10.7$ (c 0.75, CHCl_3).

4.1.3.20. (3R,4R)-3-(4-Benzylloxy-3-methoxybenzyl)-4-(3,4-diethoxybenzyl)dihydrofuran-2-one (14f). By the procedure similar to preparation of **14a**, **14f** was prepared from **13d** and 4-benzylloxy-3-methoxybenzyl bromide [20] (48%) as a pale yellow oil: ^1H NMR (300 MHz, CDCl_3) δ : 1.41–1.59 (6H, m), 2.43–2.63 (4H, m), 2.91–2.95 (2H, m), 3.82–3.90 (1H, m), 3.85 (3H, s), 3.82–3.89 (1H, m), 3.97–4.12 (5H, m), 5.12 (2H, s), 6.49–6.80 (6H, m), 7.26–7.44 (5H, m); ^{13}C NMR (75 MHz, CDCl_3) δ : 14.85, 34.50, 38.07, 41.12, 46.50, 55.96, 64.59, 71.09, 71.21, 112.90, 113.63, 114.06, 114.20, 120.78, 121.33, 127.26, 127.81, 128.51, 130.50, 130.86, 137.12, 147.06, 147.60, 148.77, 149.76, 178.70; IR (neat): 1509 (C=C), 1772 (C=O) cm^{-1} ; MS (EI) m/z 490 (M^+); HRMS (EI): calcd for $\text{C}_{30}\text{H}_{34}\text{O}_6$: 490.2355 (M^+), found: 490.2388; $[\alpha]_{\text{D}}^{25} -13.5$ (c 0.98, CHCl_3).

4.1.3.21. (3R,4R)-3-(4-Benzylloxy-3-ethoxybenzyl)-4-(3,4-diethoxybenzyl)dihydrofuran-2-one (14g). By the procedure similar to preparation of **14a**, **14g** was prepared from **13d** and 4-benzylloxy-3-ethoxybenzyl bromide [21] (56%) as a pale yellow oil: ^1H NMR

(300 MHz, CDCl₃) δ : 1.41–1.44 (9H, m), 2.42–2.60 (4H, m), 3.82–3.86 (1H, m), 4.02–4.13 (7H, m), 5.11 (2H, s), 6.47–6.81 (6H, m), 7.27–7.44 (5H, m); ¹³C NMR (75 MHz, CDCl₃) δ : 14.87, 34.50, 38.09, 41.11, 46.50, 64.60, 71.22, 71.37, 113.63, 114.17, 114.69, 115.08, 120.79, 121.48, 127.21, 127.71, 128.42, 130.53, 131.07, 137.35, 147.41, 147.95, 148.78, 149.32, 178.73; IR (neat): 1514 (C=C), 1770 (C=O) cm⁻¹; MS (EI) m/z 504 (M⁺); HRMS (EI): calcd for C₃₁H₃₆O₆: 504.2512 (M⁺), found: 504.6139; [α]_D²⁵ –12.0 (c 0.58, CHCl₃).

4.1.3.22. (3*R*,4*R*)-3-(4-Benzoyloxy-3-propoxybenzyl)-4-(4-methoxy-3-propoxybenzyl)dihydrofuran-2-one (**14h**). By the procedure similar to preparation of **14a**, **14h** was prepared from **13e** and 4-benzoyloxy-3-propoxybenzyl bromide (49%) as a pale yellow oil: ¹H NMR (400 MHz, CDCl₃) δ : 1.02–1.08 (6H, m), 1.82–1.88 (4H, m), 2.45–2.63 (4H, m), 2.85–2.97 (2H, m), 3.83 (3H, s), 3.83–4.60 (6H, m), 5.10 (2H, s), 6.51–6.96 (6H, m), 7.28–7.45 (5H, m); ¹³C NMR (100 MHz, CDCl₃) δ : 10.48, 14.84, 22.56, 34.46, 38.00, 41.07, 46.45, 64.71, 65.15, 70.55, 70.74, 71.18, 71.35, 71.37, 112.76, 114.42, 115.12, 119.34, 120.77, 121.40, 127.13, 127.15, 127.64, 128.34, 128.36, 130.63, 131.13, 137.36, 147.98, 149.58, 178.73; IR (neat): 1514 (C=C), 1771 (C=O) cm⁻¹; MS (EI) m/z 518 (M⁺); HRMS (EI): calcd for C₃₂H₃₈O₆: 518.2668 (M⁺), found: 518.2669; [α]_D²⁵ –12.2 (c 0.75, CHCl₃).

4.1.3.23. (3*R*,4*R*)-3-(4-Benzoyloxy-3-propoxybenzyl)-4-(4-ethoxy-3-propoxybenzyl)dihydrofuran-2-one (**14i**). By the procedure similar to preparation of **14a**, **14i** was prepared from **13f** and 4-benzoyloxy-3-propoxybenzyl bromide (33%) as a pale yellow oil: ¹H NMR (400 MHz, CDCl₃) δ : 1.02–1.08 (6H, m), 1.41 (3H, t, J = 7.1 Hz), 1.80–1.91 (4H, m), 2.41–2.63 (4H, m), 2.87–2.94 (2H, m), 3.82–3.96 (5H, m), 4.01 (2H, q, J = 7.1 Hz), 4.05–4.10 (1H, m), 5.10 (2H, s), 6.49–6.96 (6H, m), 7.28–7.45 (5H, m); ¹³C NMR (100 MHz, CDCl₃) δ : 10.50, 22.59, 34.51, 38.05, 41.12, 46.48, 56.00, 65.22, 70.57, 71.40, 111.86, 112.79, 113.63, 114.72, 115.30, 119.36, 120.55, 121.40, 127.16, 127.28, 127.65, 128.36, 130.41, 131.16, 137.37, 147.43, 148.25, 148.58, 149.62, 178.70; IR (neat): 1508 (C=C), 1767 (C=O) cm⁻¹; MS (EI) m/z 532 (M⁺); HRMS (EI): calcd for C₃₃H₄₀O₆: 532.2825 (M⁺), found: 518.2817; [α]_D²⁵ –6.3 (c 0.80, CHCl₃).

4.1.3.24. (3*R*,4*R*)-4-(3-Ethoxy-4-methoxybenzyl)-3-(4-hydroxy-3-methoxybenzyl)dihydrofuran-2-one (**4g**). To a stirred solution of **14a** (47.5 mg, 0.10 mmol) in MeOH (5 mL) was added 20% Pd(OH)₂ (20 mg), and the resulting suspension was stirred under a hydrogen atmosphere at 1 atm for 20 h. The catalyst was removed by filtration and the filtrate was evaporated to give a residue, which was chromatographed on silica gel (10 g, hexane:acetone = 3:1) to give **4g** (34.1 mg, 89%) as a pale yellow oil: ¹H NMR (300 MHz, CDCl₃) δ : 1.45 (3H, t, J = 7.1 Hz), 2.43–2.65 (4H, m), 2.91–2.94 (2H, m), 3.81–3.89 (1H, m), 3.83 (3H, s), 3.84 (3H, s), 4.01 (2H, q, J = 7.1 Hz), 4.12 (1H, dd, J = 9.1, 6.9 Hz), 5.53 (1H, s), 6.47–6.65 (4H, m), 6.69 (1H, d, J = 8.0 Hz), 6.82 (1H, d, J = 8.0 Hz); ¹³C NMR (75 MHz, CDCl₃) δ : 14.80, 30.91, 34.46, 38.09, 40.95, 46.55, 55.83, 55.94, 64.30, 71.27, 99.88, 111.54, 113.26, 114.10, 120.58, 122.08, 129.47, 130.35, 144.52, 146.67, 148.11, 148.33; IR (neat): 1513 (C=C), 1771 (C=O) cm⁻¹; MS (EI) m/z 386 (M⁺); HRMS (EI): calcd for C₂₂H₂₆O₆: 386.1729 (M⁺), found: 386.1693; [α]_D²⁵ –17.2 (c 1.44, CHCl₃).

4.1.3.25. (3*R*,4*R*)-4-(3-Ethoxy-4-hydroxybenzyl)-3-(3-ethoxy-4-methoxybenzyl)dihydrofuran-2-one (**4h**). By the procedure similar to preparation of **4g**, **4h** was prepared from **14b** (63%) as a pale yellow oil: ¹H NMR (300 MHz, CDCl₃) δ : 1.42–1.47 (6H, m), 2.46–2.63 (4H, m), 2.92 (2H, d, J = 5.8 Hz), 3.81–3.89 (1H, m), 3.84 (3H, s), 3.97–4.12 (5H, m), 5.60 (1H, br), 6.48–6.84 (6H, m); ¹³C NMR (75 MHz, CDCl₃) δ : 14.78, 30.88, 34.39, 38.04, 40.90, 46.53, 55.90, 64.26, 64.39, 71.24, 111.51, 112.37, 113.21, 114.01, 120.55, 121.95, 129.34, 130.35, 144.59, 145.93, 148.08, 148.03, 178.74; IR

(neat): 1516 (C=C), 1768 (C=O) cm⁻¹; MS (EI) m/z 400 (M⁺); HRMS (EI): calcd for C₂₃H₂₈O₆: 400.1886 (M⁺), found: 400.1868; [α]_D²⁷ –16.9 (c 1.13, CHCl₃).

4.1.3.26. (3*R*,4*R*)-4-(4-Ethoxy-3-methoxybenzyl)-3-(4-hydroxy-3-methoxybenzyl)dihydrofuran-2-one (**4i**). By the procedure similar to preparation of **4g**, **4i** was prepared from **14c** (57%) as a pale yellow oil: ¹H NMR (300 MHz, CDCl₃) δ : 1.45 (3H, t, J = 7.1 Hz), 2.44–2.67 (4H, m), 2.93 (2H, d, J = 5.8 Hz), 3.81 (3H, s), 3.82 (3H, s), 3.84–3.99 (1H, m), 4.03–4.15 (1H, m), 4.08 (2H, q, J = 7.1 Hz), 5.30 (1H, br), 6.47–6.66 (4H, m), 6.75 (1H, d, J = 8.0 Hz), 6.82 (1H, d, J = 8.0 Hz); ¹³C NMR (75 MHz, CDCl₃) δ : 14.90, 30.99, 34.53, 38.22, 40.97, 46.63, 55.89, 64.35, 71.31, 111.48, 112.00, 112.71, 114.04, 120.47, 122.01, 129.37, 130.30, 144.39, 146.54, 146.99, 149.18, 178.56; IR (neat): 1749 (C=O), 3648 (OH) cm⁻¹; MS (EI) m/z 386 (M⁺); HRMS (EI): calcd for C₂₂H₂₆O₆: 386.1729 (M⁺), found: 386.1693; [α]_D²⁶ –9.5 (c 0.71, CHCl₃).

4.1.3.27. (3*R*,4*R*)-4-(3-Ethoxy-4-hydroxybenzyl)-3-(4-ethoxy-3-methoxybenzyl)dihydrofuran-2-one (**4j**). By the procedure similar to preparation of **4g**, **4j** was prepared from **14d** (63%) as a pale yellow oil: ¹H NMR (300 MHz, CDCl₃) δ : 1.39–1.46 (6H, m), 2.41–2.66 (4H, m), 2.91 (2H, d, J = 6.0 Hz), 3.80 (3H, s), 3.81–3.87 (1H, m), 4.00–4.10 (5H, m), 5.64 (1H, br), 6.47–6.65 (4H, m), 6.74 (1H, d, J = 8.2 Hz), 6.82 (1H, d, J = 8.2 Hz); ¹³C NMR (75 MHz, CDCl₃) δ : 14.75, 30.86, 34.35, 38.06, 40.84, 46.54, 55.78, 64.26, 64.37, 71.24, 111.98, 112.38, 112.69, 114.00, 120.52, 121.95, 129.32, 130.38, 144.58, 145.91, 147.07, 149.25; IR (neat): 1771 (C=O), 3548 (OH) cm⁻¹; MS (EI) m/z 400 (M⁺); HRMS (EI): calcd for C₂₃H₂₈O₆: 400.1886 (M⁺), found: 400.1897; [α]_D²⁶ –12.4 (c 1.04, CHCl₃).

4.1.3.28. (3*R*,4*R*)-4-(3-Ethoxy-4-methoxybenzyl)-3-(4-hydroxy-3-propoxybenzyl)dihydrofuran-2-one (**4k**). By the procedure similar to preparation of **4g**, **4k** was prepared from **14e** (56%) as a pale yellow oil: ¹H NMR (400 MHz, CDCl₃) δ : 1.04 (3H, t, J = 7.4 Hz), 1.45 (3H, t, J = 7.1 Hz), 1.82 (2H, sextet, J = 7.4 Hz), 2.48–2.63 (4H, m), 2.91 (2H, d, J = 5.9 Hz), 3.81–3.88 (4H, m), 3.93 (2H, t, J = 7.4 Hz), 4.02 (2H, q, J = 7.1 Hz), 4.06–4.12 (1H, m), 5.57 (1H, s), 6.48 (1H, s), 6.54 (1H, d, J = 10.2 Hz), 6.60 (1H, d, J = 10.2 Hz), 6.66 (1H, s), 6.75 (1H, d, J = 8.2 Hz), 6.82 (1H, d, J = 8.2 Hz); ¹³C NMR (100 MHz, CDCl₃) δ : 10.43, 14.79, 22.49, 34.41, 38.05, 40.95, 46.54, 55.92, 64.29, 70.32, 71.24, 111.55, 112.43, 113.26, 114.01, 120.57, 121.93, 129.37, 130.37, 144.64, 146.05, 148.12, 148.33, 178.75; IR (neat): 1516 (C=C), 1769 (C=O), 3589 (OH) cm⁻¹; MS (EI) m/z 414 (M⁺); HRMS (EI): calcd for C₂₄H₃₀O₆: 414.2042 (M⁺), found: 414.2046; [α]_D²⁶ –10.6 (c 1.10, CHCl₃).

4.1.3.29. (3*R*,4*R*)-4-(3,4-Diethoxybenzyl)-3-(4-hydroxy-3-methoxybenzyl)dihydrofuran-2-one (**4l**). By the procedure similar to preparation of **4g**, **4l** was prepared from **14f** (81%) as a pale yellow oil: ¹H NMR (300 MHz, CDCl₃) δ : 1.25–1.45 (6H, m), 2.44–2.66 (4H, m), 2.92 (2H, d, J = 6.0 Hz), 3.83 (3H, s), 3.85–3.89 (1H, m), 3.98–4.13 (5H, m), 5.55 (1H, br), 6.49–6.67 (4H, m), 6.76 (1H, d, J = 7.8 Hz), 6.82 (1H, d, J = 7.8 Hz); ¹³C NMR (75 MHz, CDCl₃) δ : 14.84, 30.91, 34.40, 38.04, 40.94, 46.56, 55.84, 64.58, 71.25, 111.56, 113.60, 114.11, 120.77, 122.10, 129.47, 130.51, 144.51, 146.65, 147.57, 148.78, 178.75; IR (neat): 1766 (C=O), 2978 (OH) cm⁻¹; MS (EI) m/z 400 (M⁺); HRMS (EI): calcd for C₂₃H₂₈O₆: 400.1886 (M⁺), found: 400.1858; [α]_D²⁷ –16.0 (c 1.33, CHCl₃).

4.1.3.30. (3*R*,4*R*)-4-(3,4-Diethoxybenzyl)-3-(4-hydroxy-3-ethoxybenzyl)dihydrofuran-2-one (**4m**). By the procedure similar to preparation of **4g**, **4m** was prepared from **14g** (66%) as a pale yellow oil: ¹H NMR (300 MHz, CDCl₃) δ : 1.40–1.46 (9H, m), 2.42–2.67 (4H, m), 2.91 (2H, d, J = 5.7 Hz), 3.85 (1H, dd, J = 9.1, 7.4 Hz), 3.97–4.12

(7H, m), 5.59 (1H, br), 6.49–6.66 (4H, m), 6.75 (1H, d, $J = 8.0$ Hz), 6.82 (1H, d, $J = 8.0$ Hz); ^{13}C NMR (75 MHz, CDCl_3) δ : 14.81, 14.85, 34.39, 38.06, 40.92, 46.58, 64.42, 64.59, 71.27, 112.43, 113.62, 114.05, 114.10, 120.80, 122.00, 129.37, 130.53, 144.61, 145.94, 147.58, 148.80, 178.79; IR (neat): 1516 ($\text{C}=\text{C}$), 1761 ($\text{C}=\text{O}$) cm^{-1} ; MS (EI) m/z 414 (M^+); HRMS (EI): calcd for $\text{C}_{24}\text{H}_{30}\text{O}_6$: 414.2042 (M^+), found: 414.2024; $[\alpha]_{\text{D}}^{25} -14.0$ (c 0.70, CHCl_3).

4.1.3.31. (3*R*,4*R*)-4-(4-Methoxy-3-propoxybenzyl)-3-(4-hydroxy-3-propoxybenzyl)dihydrofuran-2-one (**4n**). By the procedure similar to preparation of **4g**, **4n** was prepared from **14h** (46%) as a pale yellow oil: ^1H NMR (400 MHz, CDCl_3) δ : 1.02–1.07 (6H, m), 1.78–1.90 (4H, m), 2.47–2.65 (4H, m), 2.92 (2H, d, $J = 5.9$ Hz), 3.81 (3H, s), 3.81–3.95 (5H, m), 4.08–4.12 (1H, m), 5.56 (1H, br), 6.50 (1H, s), 6.53 (1H, d, $J = 7.9$ Hz), 6.60 (1H, d, $J = 7.9$ Hz), 6.66 (1H, s), 6.75 (1H, d, $J = 8.2$ Hz), 6.82 (1H, d, $J = 8.2$ Hz); ^{13}C NMR (100 MHz, CDCl_3) δ : 10.39, 22.45, 22.47, 34.37, 38.01, 40.91, 46.54, 56.00, 70.29, 70.48, 71.23, 77.21, 111.81, 112.43, 113.53, 114.00, 120.55, 121.90, 129.34, 130.41, 144.61, 146.03, 148.22, 148.58, 178.74; IR (neat): 1516 ($\text{C}=\text{C}$), 1767 ($\text{C}=\text{O}$), 3422 (OH) cm^{-1} ; MS (EI) m/z 428 (M^+); HRMS (EI): calcd for $\text{C}_{25}\text{H}_{32}\text{O}_6$: 428.2199 (M^+), found: 428.2216; $[\alpha]_{\text{D}}^{25} -13.7$ (c 0.70, CHCl_3).

4.1.3.32. (3*R*,4*R*)-4-(4-Ethoxy-3-propoxybenzyl)-3-(4-hydroxy-3-propoxybenzyl)dihydrofuran-2-one (**4o**). By the procedure similar to preparation of **4g**, **4o** was prepared from **14i** (63%) as a pale yellow oil: ^1H NMR (400 MHz, CDCl_3) δ : 1.02–1.07 (6H, m), 1.42 (3H, t, $J = 7.1$ Hz), 1.80–1.86 (4H, m), 2.41–2.63 (4H, m), 2.92 (2H, d, $J = 5.9$ Hz), 3.83–3.96 (5H, m), 4.01 (2H, q, $J = 7.1$ Hz), 4.07–4.11 (1H, m), 5.57 (1H, s), 6.51–6.84 (6H, m); ^{13}C NMR (100 MHz, CDCl_3) δ : 10.50, 22.59, 34.51, 38.05, 41.12, 46.48, 56.00, 65.22, 70.57, 71.40, 111.86, 112.79, 113.63, 114.72, 115.30, 119.36, 120.55, 121.40, 127.16, 127.28, 127.65, 128.36, 130.41, 131.16, 137.37, 147.43, 148.25, 148.58, 149.62, 178.7010.45, 148.7, 22.50, 22.60, 34.37, 38.04, 40.92, 46.58, 64.76, 70.33, 70.76, 71.26, 100.36, 112.48, 114.02, 114.06, 114.38, 129.37, 130.67, 144.63, 146.04, 147.70, 149.14; IR (neat): 1508 ($\text{C}=\text{C}$), 1770 ($\text{C}=\text{O}$) cm^{-1} ; MS (EI) m/z 442 (M^+); HRMS (EI): calcd for $\text{C}_{26}\text{H}_{34}\text{O}_6$: 442.2355 (M^+), found: 442.2350; $[\alpha]_{\text{D}}^{25} -12.9$ (c 0.50, CHCl_3).

4.1.4. Effective synthesis of (3*R*,4*R*)-4-(3,4-diethoxybenzyl)-3-(4-hydroxy-3-ethoxybenzyl)dihydrofuran-2-one (**4m**)

4.1.4.1. 2-(3,4-Diethoxybenzyl)malonic acid diethyl ester (**17**). To a stirred solution of (3,4-diethoxyphenyl)methanol (**16**) [16.23] (733 mg, 3.74 mmol) in CH_2Cl_2 (20 mL) were added NEt_3 (0.67 mL, 4.86 mmol) and MsCl (0.32 mL, 4.11 mmol) at 0 °C, and the reaction mixture was stirred at room temperature for 0.5 h. The reaction was quenched with sat. NaHCO_3 (aq) (10 mL), and the organic layer were separated. The aqueous layer was extracted with CH_2Cl_2 (20 mL \times 3), and the organic layer and extracts were combined, dried over MgSO_4 . The solvent was removed under reduced pressure to give a pale yellow oil, which was used directly in the next step. To a stirred solution of diethyl malonate (1.14 mL, 7.48 mmol) in DMF (20 mL) was added NaH (60%, 299 mg, 7.48 mmol) at 0 °C, and the resulting mixture was stirred at room temperature for 1 h. To the solution was added a solution of the oil obtained above in DMF (2 mL) at 0 °C, and the reaction mixture was stirred at room temperature for 25 h. The reaction was quenched with sat. NaHCO_3 (aq) (10 mL), and the aqueous mixture was extracted with Et_2O (20 mL \times 3). The organic extracts were combined, dried over MgSO_4 , evaporated to give a pale yellow oil which was chromatographed on silica gel (20 g, hexane:acetone = 15:1) to give **17** (1.10 g, 87% in 2 steps) as a pale yellow oil: ^1H NMR (300 MHz, CDCl_3) δ : 1.15–1.30 (6H, m), 1.39–1.46 (6H, m), 3.13 (2H, d, $J = 8.0$ Hz), 3.59 (1H, t, $J = 8.0$ Hz),

4.01–4.24 (8H, m), 6.68–6.78 (3H, m); ^{13}C NMR (75 MHz, CDCl_3) δ : 13.77, 13.83, 14.57, 14.60, 34.06, 41.37, 53.82, 61.11, 64.19, 113.33, 114.09, 120.83, 130.28, 147.28, 148.33, 166.34, 168.64; IR (neat): 1516 ($\text{C}=\text{C}$), 1731 ($\text{C}=\text{O}$) cm^{-1} ; MS (EI) m/z 338 (M^+); HRMS (EI): calcd for $\text{C}_{23}\text{H}_{28}\text{O}_6$: 338.1729 (M^+), found: 338.1766.

4.1.4.2. (*R*)-Acetic acid 3-(3,4-diethoxyphenyl)-2-hydroxymethylpropyl ester (**18**). To a stirred solution of **17** (1.43 g, 4.23 mmol) in THF (40 mL) was added LiAlH_4 (401 mg, 10.6 mmol) at 0 °C, and the resulting suspension was refluxed for 12 h. The reaction was quenched with 10% NaOH (aq) (20 mL), and the mixture was extracted with AcOEt (20 mL \times 5). The organic extracts were combined dried over MgSO_4 , and the solvent was evaporated to give diol, which was used directly in the next step. To a stirred solution of the diol obtained above in *i*-Pr $_2\text{O}$ -THF (15 mL, 4:1) were added Lipase-PS (323 mg) and vinyl acetate (0.45 mL, 4.85 mmol), and the reaction mixture was stirred at room temperature for 2 h. The catalyst was filtered and the filtrate was evaporated to give residue, which was chromatographed on silica gel (30 g, hexane:acetone = 4:1) to give **18** (669 mg, 53% in 2 steps) as a pale yellow oil. The enantiomeric excess of **18** was determined to be a 98% ee by the Mosher's method [24]. ^1H NMR (300 MHz, CDCl_3) δ : 1.39–1.44 (6H, m), 2.06 (3H, s), 2.23 (1H, br), 2.49–2.64 (2H, m), 3.45–3.59 (2H, m), 4.01–4.08 (6H, m), 4.15 (1H, dd, $J = 11.3, 4.7$ Hz), 6.66–6.70 (2H, m), 6.78 (1H, d, $J = 8.0$ Hz); ^{13}C NMR (75 MHz, CDCl_3) δ : 14.88, 20.91, 33.86, 42.53, 62.07, 64.03, 64.55, 64.63, 113.69, 114.52, 121.22, 131.91, 147.23, 148.70, 171.68; IR (neat): 1513 ($\text{C}=\text{C}$), 1721 ($\text{C}=\text{O}$) cm^{-1} ; MS (EI) m/z 296 (M^+); HRMS (EI): calcd for $\text{C}_{16}\text{H}_{24}\text{O}_5$: 296.1624 (M^+), found: 296.1594; $[\alpha]_{\text{D}}^{28} +18.8$ (c 1.47, CHCl_3); 98% ee.

4.1.4.3. (*R*)-Acetic acid 3-(3,4-Diethoxyphenyl)-2-methanesulfonyloxymethylpropyl ester (**19**). To a stirred solution of **18** (1.45 g, 4.96 mmol) in CH_2Cl_2 (25 mL) were added MsCl (0.42 mL, 5.45 mmol) and NEt_3 (0.89 mL, 6.45 mmol) at 0 °C, and the reaction mixture was stirred at room temperature for 0.5 h. The reaction was quenched with H_2O (20 mL), and the aqueous mixture was extracted with CH_2Cl_2 (20 mL \times 3). The organic extracts were combined dried over MgSO_4 , and evaporated. The residue was chromatographed on silica gel (40 g, hexane:acetone = 4:1) to give **19** (1.48 g, 79%) as a pale yellow oil: ^1H NMR (300 MHz, CDCl_3) δ : 1.41–1.46 (6H, m), 2.08 (3H, s), 2.32–2.36 (1H, m), 2.65 (2H, d, $J = 7.4$ Hz), 2.99 (3H, s), 4.00–4.23 (8H, m), 6.65–6.70 (2H, m), 6.80 (1H, d, $J = 8.0$ Hz); ^{13}C NMR (75 MHz, CDCl_3) δ : 14.85, 20.81, 30.90, 33.49, 37.21, 39.71, 63.02, 64.60, 68.48, 113.70, 114.40, 121.22, 130.36, 147.53, 148.82, 170.78; IR (neat): 1512 ($\text{C}=\text{C}$), 1735 ($\text{C}=\text{O}$) cm^{-1} ; MS (EI) m/z 374 (M^+); HRMS (EI): calcd for $\text{C}_{17}\text{H}_{26}\text{O}_7\text{S}$: 374.1399 (M^+), found: 374.1362; $[\alpha]_{\text{D}}^{25} +2.1$ (c 0.68, CHCl_3).

4.1.4.4. (*R*)-4-(3,4-Diethoxybenzyl)dihydrofuran-2-one (**13d**) from **19**. To a stirred solution of **19** (1.12 g, 3.00 mmol) in DMSO (25 mL) was added KCN (205 mg, 3.00 mmol), and the resulting mixture was heated at 90 °C for 3 h. After cooling, the reaction was quenched with H_2O (25 mL), and the aqueous mixture was extracted with $\text{Et}_2\text{O}/\text{AcOEt}$ (1:1, 20 mL \times 3). The organic extracts were combined, dried over MgSO_4 , and evaporated to give cyanide, which was used directly in the next step. To a stirred solution of cyanide obtained above in THF- H_2O (3:1, 12 mL) was added $\text{LiOH}\cdot\text{H}_2\text{O}$ (126 mg, 3.00 mmol), and the reaction mixture was stirred at room temperature for 24 h. The reaction mixture was diluted with H_2O (10 mL), and the aqueous mixture was extracted with Et_2O (20 mL \times 3). The organic extracts were combined, dried over MgSO_4 , and evaporated to give alcohol, which was used directly in the next step. The alcohol obtained above was dissolved in 10% NaOH (aq) (15 mL), and the mixture was refluxed for 5 h. After cooling, 10% HCl (aq) (30 mL) and THF (30 mL) were added to

the reaction mixture, and the resulting solution was stirred at room temperature for 50 h. The aqueous reaction mixture was extracted with Et₂O (30 mL × 3), and the organic extracts were combined, dried over MgSO₄, and evaporated to give a residue, which was chromatographed on silica gel (30 g, hexane:acetone = 3:1) to give **13d** (475 mg, 60% in 3 steps) as a pale yellow oil.

4.2. In vitro preferential cytotoxicity

4.2.1. Cells and culture

Human pancreatic cancer cell lines, PANC-1 and CAPAN-1, were maintained in Dulbecco's modified Eagle's medium (DMEM, Nissui Pharmaceutical Co., Ltd., Tokyo, Japan) supplemented with 10% fetal bovine serum (FBS, Gibco BRL Products, Gaithersburg, MD, USA), 0.1% sodium bicarbonate (Nacalai Tesque Inc.), and 1% antibiotic-antimycotic solution (Sigma–Aldrich Inc., St. Louis, MO, USA). Nutrient deprived medium (NDM) contained 265 mg/L CaCl₂·2H₂O, 0.1 mg/L Fe(NO₃)₃·9H₂O, 400 mg/L KCl, 200 mg/L MgSO₄·7H₂O, 6400 mg/L NaCl, 700 mg/L NaHCO₃, 125 mg/L NaH₂PO₄, 15 mg/L phenol red, 1 M HEPES buffer (pH 7.4, Wako Pure Chemical Industries, Ltd., Osaka, Japan), and 10 mL MEM vitamin solution (Life Technologies, Inc., Rockville, MD, USA). The final pH was adjusted to 7.4 with 10% NaHCO₃. For amino acid supplementation, stock solutions (200 mmol/L L-glutamine solution, MEM amino acids solution, and MEM nonessential amino acids solution; Life Technologies) were added at a concentration of 1%.

4.2.2. Preferential cytotoxicity

Preferential cytotoxicity was determined as previously described [9]. In brief, PANC-1 or CAPAN-1 cells (2 × 10⁴ cells/well) were seeded in 96-well plates (Corning Inc., Corning, NY, USA) and incubated in fresh DMEM at 37 °C under 5% CO₂ and 95% air for 24 h. The cells were washed with Dulbecco's phosphate-buffered saline (PBS, Nissui Pharmaceutical Co., Ltd., Tokyo, Japan) before the medium was replaced with either DMEM or NDM (for CAPAN-1, amino acids-supplemented NDM) containing serial dilutions of the test samples. After 24 h of incubation, the cells were washed with PBS, and 100 μL of DMEM containing 10% WST-8 cell counting kit solution (Dojindo, Kumamoto, Japan) was added to the wells. After 3 h of incubation, the absorbance was measured at 450 nm. Cell viability was calculated from the mean values for three wells using the following equation:

$$\text{Cell viability (\%)} = \frac{[\text{Abs}(\text{test samples}) - \text{Abs}(\text{blank})]}{[\text{Abs}(\text{control}) - \text{Abs}(\text{blank})]} \times 100$$

The preferential cytotoxicity was expressed as the concentration at which 50% of cells died preferentially in NDM (PC₅₀).

4.3. In vivo antitumor activity of triethoxy derivative **4m** in nude mice

Five-week-old female BALB/cAJcl-*nu/nu* mice were obtained from CLEA Japan, Inc. (Tokyo, Japan), and 5 × 10⁶ CAPAN-1 cells in 0.3 mL DMEM were s.c. injected into the right side of the back of the animals. Two weeks later, 12 mice bearing tumors around 5 mm in diameter were randomly divided into treatment groups and a vehicle control group. Because (–)-arctigenin (**1**) and triethoxy derivative **4m** are poorly soluble in water, they were first dissolved in DMSO at 10 mg/mL and kept frozen until use. Just before administration, the stock solution was diluted in saline to a final concentration of 250 μg/mL (the final concentration of DMSO in saline is 2.5%). The mice were administered by *i.p.*-injections of 0.2 mL of solution of arctigenin, triethoxy derivative **4m**, or vehicle on 6 days of the week for 4 weeks. The tumor size and body weight were measured weekly and the tumor volume was calculated using the following formula: Tumor volume = $\frac{4}{3} \times 3.14 \times (L/2 \times W/2 \times W/2)$ where *L* is the length of the tumor and *W* is its width.

Results are expressed as means ±SD. Statistical comparisons were conducted using Student's *t* test after ANOVA. The results were considered to be significant when *P* < 0.05.

Acknowledgments

This work was supported in part by grants from the Ministry of Health and Welfare for the Third-Term Comprehensive 10-Year Strategy for Cancer Control and by Grant-in-Aid for Scientific Research (C) (No. 22590098) from Japan Society for the Promotion of Science (JSPS).

Appendix A. Supplementary data

Supplementary data related to this article can be found at <http://dx.doi.org/10.1016/j.ejmech.2012.11.031>.

References

- [1] J. Ferlay, H.R. Shin, F. Bray, D. Forman, C. Mathers, D.M. Parkin, GLOBOCAN 2008 v1.2, Cancer Incidence and Mortality Worldwide: IARC CancerBase No. 10 (Internet), International Agency for Research on Cancer, Lyon, France, 2010, Available from: <http://globocan.iarc.fr> (accessed 08.05.12).
- [2] D. Li, K. Xie, R. Wolff, J.L. Abbruzzese, Pancreatic cancer, *Lancet* 363 (2004) 1049–1057.
- [3] S. Shore, D. Vimalachandran, M.G.T. Raraty, P. Ghaneh, Cancer in the elderly: pancreatic cancer, *Surg. Oncol.* 13 (2004) 201–210.
- [4] H.W. Chung, S.M. Bang, S.W. Park, J.B. Chung, J.K. Kang, J.W. Kim, J.S. Seong, W.J. Lee, S.Y. Song, A prospective randomized study of gemcitabine with doxifluridine versus paclitaxel with doxifluridine in concurrent chemoradiotherapy for locally advanced pancreatic cancer, *Int. J. Radiat. Oncol.* 60 (2004) 1494–1501.
- [5] C.V. Dang, G.L. Semenza, Oncogenic alteration of metabolism, *Trends Biochem. Sci.* 24 (1999) 68–72.
- [6] M. Kitano, M. Kudo, K. Maekawa, Y. Suetomi, H. Sakamoto, N. Fukuta, R. Nakaoka, T. Kawasaki, Dynamic imaging of pancreatic diseases by contrast enhanced coded phase inversion harmonic ultrasonography, *Gut* 53 (2004) 854–859.
- [7] K. Izuishi, K. Kato, T. Ogura, T. Kinoshita, H. Esumi, Remarkable tolerance of tumor cells to nutrient deprivation: possible new biochemical target for cancer therapy, *Cancer Res.* 60 (2000) 6201–6207.
- [8] (a) H. Esumi, J. Lu, Y. Kurashima, T. Hanaoka, Antitumor activity of pyrinium pamoate, 6-(dimethylamino)-2-[2-(2,5-dimethyl-1-phenyl-1H-pyrrol-3-yl)ethenyl]-1-methyl-quinolinium pamoate salt, showing preferential cytotoxicity during glucose starvation, *Cancer Sci.* 95 (2004) 685–690; (b) J. Lu, S. Kunimoto, Y. Yamazaki, M. Kaminishi, H. Esumi, D. Kigamicin, A novel anticancer agent based on a new anti-austerity strategy targeting cancer cells' tolerance to nutrient starvation, *Cancer Sci.* 95 (2004) 547–552.
- [9] S. Awale, J. Lu, S.K. Kalauni, Y. Kurashima, Y. Tezuka, S. Kadota, H. Esumi, Identification of arctigenin as an antitumor agent having the ability to eliminate the tolerance of cancer cells to nutrient starvation, *Cancer Res.* 66 (2006) 1751–1757.
- [10] (a) B. Hausott, H. Greger, B. Marian, Naturally occurring lignans efficiently induce apoptosis in colorectal tumor cells, *J. Cancer Res. Clin. Oncol.* 129 (2003) 569–576; (b) T. Matsumoto, K. Hosono-Nishiyama, H. Yamada, Antiproliferative and apoptotic effects of butyrolactone lignans from *Arctium lappa* on leukemic cells, *Planta Med.* 72 (2006) 276–278; (c) T. Toyoda, T. Tsukamoto, T. Mizoshita, S. Nishibe, T. Deyama, Y. Takenaka, N. Hirano, H. Tanaka, S. Takasu, H. Ban, T. Kumagai, K. Inada, H. Utsunomiya, M. Tatematsu, Inhibitory effect of nordihydroguaiaretic acid, a plant lignan, on *Helicobacter pylori*-associated gastric carcinogenesis in Mongolian gerbils, *Cancer Sci.* 98 (2007) 1689–1695.
- [11] (a) M. Nose, T. Fujimoto, T. Takeda, S. Nishibe, Y. Ogihara, Structural transformation of lignan compounds in rat gastrointestinal tract, *Planta Med.* 58 (1992) 520–523; (b) S. Heinonen, T. Nurmi, K. Liukkonen, K. Poutanen, K. Wähälä, T. Deyama, S. Nishibe, H. Adlercreutz, In vitro metabolism of plant lignans: new precursors of mammalian lignans enterolactone and enterodiol, *J. Agr. Food Chem.* 49 (2001) 3178–3186; (c) L.-H. Xie, E.-M. Ahn, T. Akao, A.A. Abdel-Hafez, N. Nakamura, M. Hattori, Transformation of arctiin to estrogenic and antiestrogenic substances by human intestinal bacteria, *Chem. Pharm. Bull.* 51 (2003) 378–384.
- [12] E. Eich, H. Pertz, M. Kaloga, J. Schulz, M.R. Pesen, A. Mazumder, Y. Pommier, (–)-Arctigenin as a lead structure for inhibitors of human immunodeficiency virus type-1 integrase, *J. Med. Chem.* 39 (1996) 86–95.
- [13] M.G. Banwell, S. Chand, G.P. Savage, An enantioselective total synthesis of the stilbenolignan (–)-aiphanol and the determination of its absolute stereochemistry, *Tetrahedron: Asymmetry* 16 (2005) 1645–1654.